*Epilepsia*, **(*):1–8, 2011
doi: 10.1111/j.1528-1167.2011.03174.x

FULL-LENGTH ORIGINAL RESEARCH

# *CDKL5* alterations lead to early epileptic encephalopathy in both genders

*†‡Jao-Shwann Liang, *Keiko Shimojima, §Rumiko Takayama, ¶Jun Natsume, *†Minobu Shichiji, †Kyoko Hirasawa, †Kaoru Imai, #Tohru Okanishi, **Seiji Mizuno, ††Akihisa Okumura, *Midori Sugawara, §Tomoshiro Ito, §Hiroko Ikeda, §Yukitoshi Takahashi, †Hirokazu Oguni, §Katsumi Imai, †Makiko Osawa, and *Toshiyuki Yamamoto

*Tokyo Women's Medical University Institute for Integrated Medical Sciences, Tokyo, Japan; †Department of Pediatrics, Tokyo Women's Medical University, Tokyo, Japan; ‡Department of Pediatrics, Far Eastern Memorial Hospital, Taipei, Taiwan; §National Epilepsy Center, Shizuoka Institute of Epilepsy and Neurological Disorders, Shizuoka, Japan; ¶Department of Pediatrics, Nagoya University School of Medicine, Nagoya, Japan; #Department of Pediatrics, Seirei Hamamatsu Hospital, Hamamatsu, Japan; **Department of Medical Genetics, Aichi Prefectural Colony Central Hospital, Kasugai, Japan; and ††Department of Pediatrics, Juntendo University School of Medicine, Tokyo, Japan

## Summary

Purpose: Genetic mutations of the cyclin-dependent kinase-like 5 gene (*CDKL5*) have been reported in patients with epileptic encephalopathy, which is characterized by intractable seizures and severe-to-profound developmental delay. We investigated the clinical relevance of *CDKL5* alterations in both genders.

Methods: A total of 125 patients with epileptic encephalopathy were examined for genomic copy number aberrations, and 119 patients with no such aberrations were further examined for *CDKL5* mutations. Five patients with Rett syndrome, who did not show methyl CpG-binding protein 2 gene (*MECP2*) mutations, were also examined for *CDKL5* mutations.

Key Findings: One male and three female patients showed submicroscopic deletions including *CDKL5*, and two male and six female patients showed *CDKL5* nucleotide alterations. Development of early onset seizure was a characteristic clinical feature for the patients with *CDKL5* alterations in both genders despite polymorphous seizure types, including myoclonic seizures, tonic seizures, and spasms. Severe developmental delays and mild frontal lobe atrophies revealed by brain magnetic resonance imaging (MRI) were observed in almost all patients, and there was no gender difference in phenotypic features.

Significance: We observed that 5% of the male patients and 14% of the female patients with epileptic encephalopathy had *CDKL5* alterations. These findings indicate that alterations in *CDKL5* are associated with early epileptic encephalopathy in both female and male patients.

KEY WORDS: *CDKL5*, Epileptic encephalopathy, Genomic copy number aberration, Mutation, Gender.

Epileptic encephalopathies are a group of conditions in which neurologic deterioration results mainly from epileptic activity. The clinical and electroencephalography (EEG) characteristics depend on the age of onset and may change over time (Zupanc, 2009). An underlying genetic background has been suggested in patients with epileptic encephalopathy (Nabbout & Dulac, 2008). An X-linked gene coding for cyclin-dependent kinase-like 5 gene (*CDKL5*; MIM #300203) is one of the genes responsible for epileptic encephalopathy. Kalscheuer et al. (2003) identified de novo balanced X autosome translocations in two female patients with infantile spasms, in whom *CDKL5* was disrupted. Since then, the phenotypic spectrum of *CDLK5* abnormalities has expanded to include features resembling Rett syndrome (RTT; MIM #312750) with early onset seizures (Evans et al., 2005; Mari et al., 2005). Now, phenotypic features of *CDLK5* abnormalities are widely recognized as early infantile epileptic encephalopathy-2 (EIEE-2; MIM #30062) and are characterized as severe epileptic encephalopathy associated with early onset and refractory seizures (Archer et al., 2006; Pintaudi et al., 2008).

Although the consequence of *CDKL5* alterations has also been attributed to X-linked dominant infantile spasm syndrome-2 (ISSX2), mutations have been identified not only in female patients but also in some male patients with severe mental retardation and early onset intractable seizures (Elia et al., 2008; Fichou et al., 2009; Sartori et al., 2009).

Accepted May 26, 2011; Early View publication Xxxxx XX, 20XX.
Address correspondence to Toshiyuki Yamamoto, Tokyo Women's Medical University Institute for Integrated Medical Sciences, 8-1 Kawada-cho, Shinjuku-ward, Tokyo 162-8666, Japan. E-mail: toshiyuki.yamamoto@twmu.ac.jp

Wiley Periodicals, Inc.

Therefore, we performed a comprehensive analysis for *CDKL5* in both female and male patients with epileptic encephalopathy.

## Methods

### Patients

After obtaining approval of the study protocol by the ethics committee of the institution and informed consent from the families of the patients, peripheral blood samples of 125 patients (59 male and 66 female) with epileptic encephalopathy of unknown etiology were collected, together with their clinical information, including neuroimaging findings. Epileptic encephalopathies are defined as disorders in which there is a temporal relationship between deterioration in cognitive, sensory, and motor function and epileptic activity, which includes frequent seizures and/or extremely frequent interictal paroxysmal activity (Nabbout & Dulac, 2003). Five female patients with RTT who did not show methyl CpG-binding protein 2 gene (*MECP2*) mutations (which are often associated with RTT) were also included in the cohort study for *CDKL5* mutations.

### Microarray-based comparative genomic hybridization (aCGH) analysis

The genomic copy numbers of the patients with epileptic encephalopathies were determined using the Human Genome CGH Microarray 105K (Agilent Technologies, Santa Clara, CA, U.S.A.) as described previously (Shimojima et al., 2010).

### Validation of the genomic copy number aberrations

Fluorescent in situ hybridization (FISH) analysis was performed for the large chromosomal deletion by using bacterial artificial chromosome (BAC) clones as probes, RP11-106N3 and CTD-2335C24 including *CDKL5* as a target, and RP11-1051J20 as a marker (Fig. 1, Table S1). The deletion identified in Patient 1 was too small to be detected by a BAC clone; therefore, multiplex polymerase chain reaction (PCR) analysis was used for validation. Two DNA fragments, exon 1B (421 bp) and exon 2 (350 bp) of *CDKL5*, were amplified in the same PCR reaction tube, separated by agarose gel electrophoresis, and visualized by ethidium bromide staining.

### Cohort study for *CDKL5*

Samples from 119 patients (58 male and 61 female) that showed no genomic copy number aberrations at the first screening by microarray-based comparative genomic hybridization (aCGH) in this study were included in the second cohort. Five samples obtained from female patients with RTT who did not show *MECP2* mutations were also included. The genomic sequences of all 23 exons of *CDKL5* were analyzed by the standard PCR direct-sequencing method using primers listed in Table S2. A recently identified exon 16B, which if included in the mature mRNA produces as a new *CDKL5* isoform, was also analyzed in this study (Fichou et al., 2010). When nucleotide changes were identified in samples for which parental samples were available, trio analyses were performed to test whether the mutation was de novo or familial. DNA samples collected from 100 healthy Japanese volunteers (50 male and 50 female) comprised the control cohort.

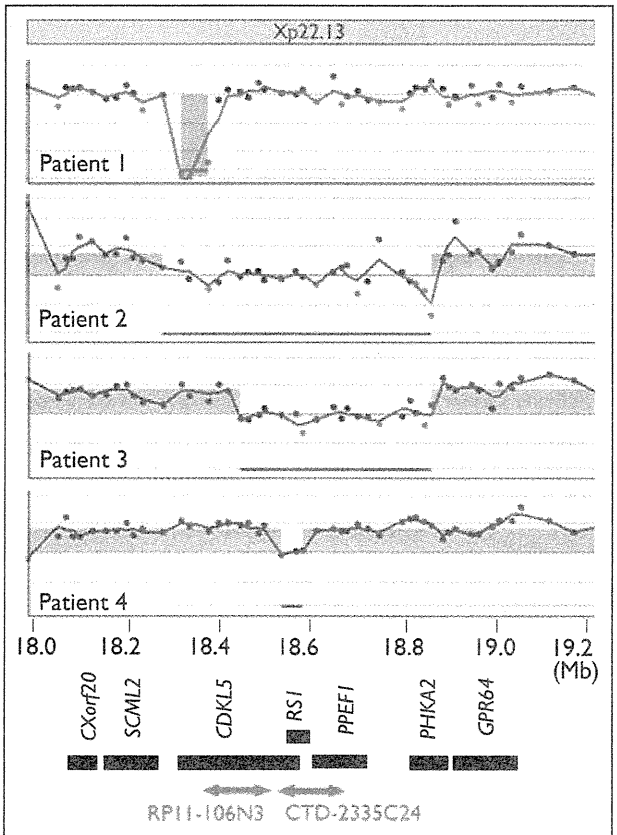


**Figure 1.**
Results of aCGH. The *CDKL5* region was expanded in Gene View with Agilent Genomic Workbench software (Agilent Technologies). The *x* and *y* axes indicate chromosomal positions and $\log_2$ ratios of intensity, respectively. Moving averages are shown in blue and red lines in male and female patients, respectively. Dots indicate the positions and $\log_2$ ratio of the probes. Rectangles and bars with arrows in both edges indicate the locations of the genes and BAC clones used for FISH, respectively. All patients show genomic copy number aberrations in the *CDKL5* region.


## Results

### Genomic copy number aberrations

In Patient 1, an aberration was identified at Xp22.13, indicating a nullisomy of this region (Fig. 1, Table S3). This region corresponds to exon 1 of *CDKL5*. Subsequent

multiplex PCR analysis using two sets of primers for exon 1B and exon 2 of *CDKL5* showed no band for exon 1B (Fig. 2A), thereby confirming the nullisomy of this region. Both parents of Patient 1 declined trio analysis.

aCGH analysis identified chromosomal aberrations in the *CDKL5* region in three female patients (Fig. 1, Table S3). Because male reference DNA was used in this study, genomic copy numbers of the normal female X chromosome regions showed $\log_2$ ratio of +1. Therefore, a $\log_2$ ratio of "0" indicates the same genomic copy numbers with the male reference sample, indicating a partial monosomy of this region in these patients. For Patients 2 and 3, identified aberrations were confirmed by FISH by detecting only one signal with RP11-106N3 and CTD-2335C24, respectively, indicating deletions in this region (Fig. 2B,C). For Patient 4, one of the targeted signals of CTD-2335C24 was weaker than the other, indicating a partial deletion of the targeted region (Fig. 2D). For Patients 2 and 3, the deletion region involved four genes: *CDKL5*; X-linked juvenile retinoschisis protein gene (*RS1*), which is responsible for X-linked juvenile retinoschisis (MIM #312700); protein phosphatase with EF hand calcium-binding gene (*PPEF1*); and phosphorylase kinase alpha 2 gene (*PHKA2*), which is responsible for X-linked hepatic glycogen storage disease (MIM #300798). For Patient 3, the deleted region involved the

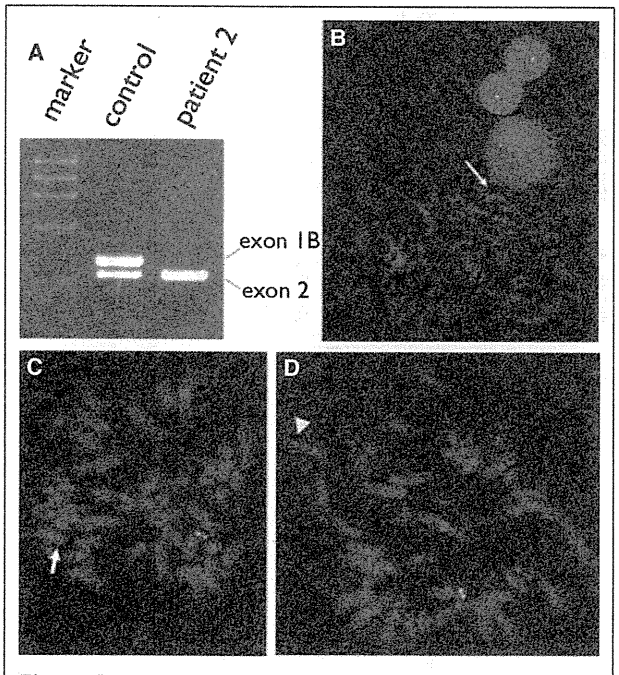


**Figure 2.**
Validations of genomic copy number aberrations. (**A**) Multiplex PCR amplification indicates deletion of exon 1B in Patient 1. The marker lane shows HaeIII digested $\varphi$X174 DNA. (**B**, **C**) FISH analysis indicates loss of the green signal on one of the X chromosomes (arrows). For Patient 2 (**B**) and Patient 3 (**C**), RP11-106N3 and CTD-2335C24 are used for the targets, respectively. Patient 4 (**D**) shows a week green signal labeled on CTD-2335C24 (arrowhead), indicating a partial deletion within CTD-2335C24 region.
*Epilepsia* © ILAE

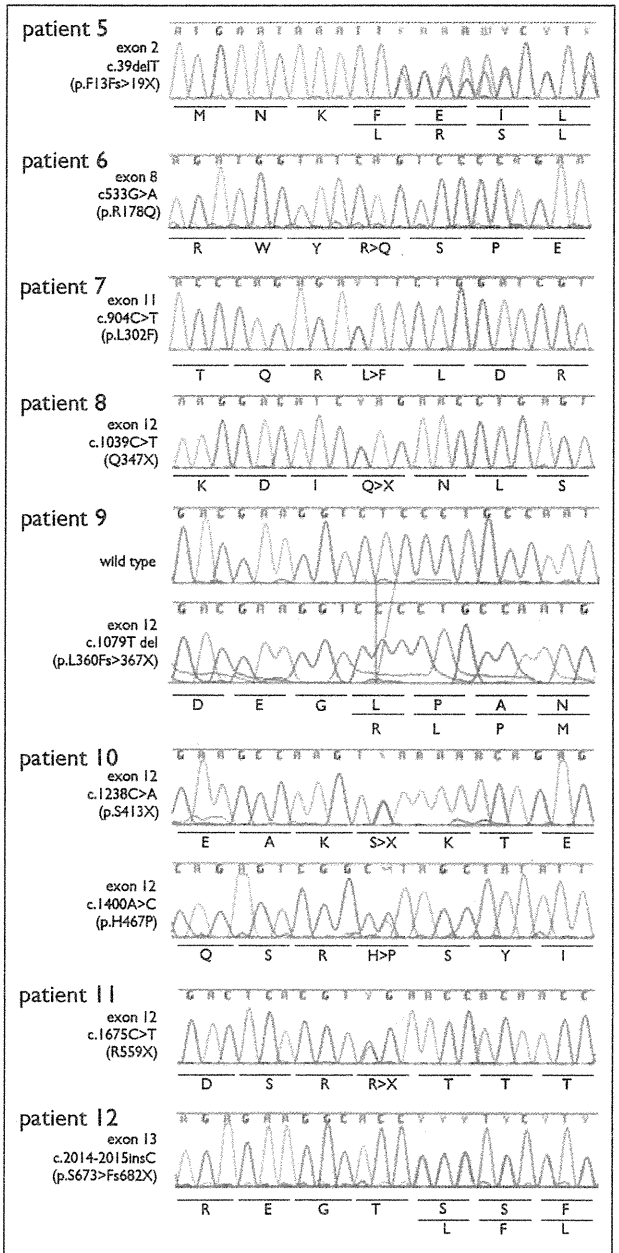


**Figure 3.**
Electrophoresis of the direct sequencing. Alphabetic symbols indicate amino acids. For Patients 5, 9, and 12, lines above the sequences indicate reference amino acid sequences, and lines below the sequences indicate amino acid changes caused by the mutations.
*Epilepsia* © ILAE

**Table 1. Summary of the clinical features and the identified *CDKL5* mutations in the patients reported in this study**

| No. | 1 | 2 | 3 | 4 | 5 | 6 | 7 | 8 | 9 | 10 | 11 | 12 |
|---|---|---|---|---|---|---|---|---|---|---|---|---|
| Gender | M | F | F | F | F | M | F | F | M | F | F | F |
| Initial concerns | EE | EE | EE | EE | EE | EE | EE | EE | EE | EE | EE | EE |
| Age at examination | 6 m | 2 y 7 m | 4 y 2 m | 2 y 7 m | 8 m | 1 y 9 m | 4 y 7 m | 2 y 6 m | 2 y | 2 y 1 m | 1 y 4 m | 1 y 4 m |
| Physical examination | | | | | | | | | | | | |
| Birth weight (g) | 3,458 | 3,016 | 2,400 | 2,716 | 2,612 | 3,800 | 2,560 | 3,352 | 3,228 | 2,955 | 3,250 | 2,976 |
| OFC at birth (cm) | 36.0 | 36.0 | 32.0 | 32.0 | 30.3 | 34.0 | NT | NT | 36.0 | NT | 33.0 | 33.5 |
| Microcephaly | – | – | + | + | + | – | – | – | – | – | – | + |
| Deceleration of head growth | – | – | – | – | + | – | – | – | – | – | – | + |
| Neurologic features | | | | | | | | | | | | |
| Hypotonia | – | – | + | + | + | + | +/– | +/– | + | +/– | + | + |
| Autistic features | NT | NT | + | NT | NT | – | +/– | + | NT | + | + | NT |
| Stereotype movement | NT | NT | + | + | + | – | – | + | NT | + | – | NT |
| Development | | | | | | | | | | | | |
| Sitting | – | – | – | – | – | – | – | + | – | – | – | + |
| Walking | – | – | – | – | – | – | – | – | – | – | – | – |
| Best motor development | Bedridden | Bedridden | Turn over | Turn over | Bedridden | Bedridden | Bedridden | Sit | Bedridden | Turn over | Turn over | Sit |
| Speech | – | – | – | – | – | – | – | – | – | – | – | – |
| Seizure | | | | | | | | | | | | |
| Age at onset of seizure | 1 m | 1 m | 2 m | 1.5 m | 2 w | 2 w | 4 d | 2 m | 3 m | 3 w | 6 m | 6 w |
| Persistent epilepsy | + | + | + | + | + | + | – | + | + | + | + | + |
| Seizure type | Infantile spasms | Infantile spasms | Spasms, focal Sz, myoclonia | Spasms, focal Sz | Spasms, focal Sz | Epileptic spasms | Infantile spasms | Tonic–clonic convulsion | Infantile spasms | Tonic–clonic convulsion | Tonic–clonic convulsion | Epileptic spasms |
| Radiologic examination | | | | | | | | | | | | |
| Brain MRI | Cerebral atrophy | Cerebral atrophy | Cerebral atrophy | Mild cerebral atrophy | Cerebral atrophy | Bifrontal-diffuse atrophy | Very mild cerebral atrophy | Mild frontal lobe atrophy | Cerebral atrophy | Cerebral atrophy | Frontal lobe atrophy and delayed myelination | Mild cerebral atrophy |
| Hypoperfusion revealed by SPECT | NT | NT | Left frontal | NT | No abnormality | Right frontal | Right temporal | Left frontal | No abnormality | NT | Frontal and left parietal | NT |

Continued

*Epilepsia*, **(*):1–8, 2011
doi: 10.1111/j.1528-1167.2011.03174.x

**Table 1. Continued**

| No. | 1 | 2 | 3 | 4 | 5 | 6 | 7 | 8 | 9 | 10 | 11 | 12 |
|---|---|---|---|---|---|---|---|---|---|---|---|---|
| Mutation | | | | | | | | | | | | |
| Location | Exon 1 | Whole exons | Large deletion after exon 4 | Large deletion after exon 16 | Exon 2 | Exon 8 | Exon 11 | Exon 12 | Exon 12 | Exon 12 | Exon 12 | Exon 13 |
| Nucleotide change | | | | | c.39delT | c.533G>A | c.904C>T | c.1039C>T | c.1079delT | c.1238C>G | c.1400A>C | c.1675C>T | c.2014-2015insC |
| Amino acid change | | | | | p.F13Fs>19X | p.R178Q | p.L302F | p.Q347X | p.L360Fs>367X | p.S413X | p.H467P | p.R559X | p.S673>Fs682X |
| Domain | | | | | | Catalytic | | | | | | | |
| Inheritance | NT | De novo | De novo | De novo | NT | De novo | NT | NT | NT | De novo | De novo | NT | De novo |
| Novel/recurrent | Novel | Novel | Novel | Novel | Novel | Novel | Novel | Recurrent | Novel | Novel | Novel | Recurrent | Novel |
| Population study | NT | NT | NT | NT | None | None | None | None | None | None | None | None | None |
| Previous reports | | | | | | | | Artuso et al. (2010) | | | | Sartori et al. (2009) | |

M, male; F, female; EE, epileptic encephalopathy; y, years; m, months; w, weeks; d, days; OFC, occipitofrontal circumference; NT, not tested; Sz, seizures; SPECT, single-photon emission computed tomography.

latter half of *CDKL5* after exon 4. Patient 4 also showed a partial *CDKL5* deletion after exon 16, and *RS1*, which was encoded in the antisense direction. For Patients 2, 3, and 4, both parents were negative for these deletions, indicating de novo origin.

There were no other known pathogenic aberrations in these four patients. In the other two patients, genomic copy number aberrations in the region of the platelet-activating factor acetylhydrolase gene (*PAFAH1B1*), which is responsible for lissencephaly, were identified (Shimojima et al., 2010). The remaining 119 patients showed no genomic copy number aberrations and were included in the cohort study for *CDKL5* mutations.

### *CDKL5* nucleotide alterations

In the 119 patients, eight pathogenic mutations were identified (including six novel and two recurrent mutations), which consisted of three nonsense mutations, three frameshift mutations, and two missense mutations (Fig. 3, Table 1). Aristaless-related homeobox gene (*ARX*; MIM #300382) was not found in any of the male patients. Five patients with RTT who did not show *MECP2* mutations also did not show mutations in *CDKL5*. No control samples showed any of the nucleotide alterations identified in this study (Table 1).

Although Patient 10 showed a nonsense mutation (p.S413X), an additional missense mutation (p.H467P) was also identified in exon 12. Neither alteration was found in parents, indicating de novo occurrence of both mutations. Because a similar missense mutation (p.H467R) was reported to be a nonpathogenic mutation, p.H467P is also expected to be a nonpathogenic mutation (Evans et al., 2005).

### Clinical description

Brain magnetic resonance imaging (MRI) of the patients with *CDKL5* alterations is shown in Fig. 4. Many patients showed frontal dominant cerebral atrophy. All clinical data including the findings of neuroimaging are summarized in Table 1. The ability to sit autonomously was the maximum gross motor development achieved by these patients, and none of the patients acquired speech ability, indicating severe developmental delay. Only the oldest patient (Patient 7; 4 years and 7 months old), who had a missense mutation, showed seizure control after 3 years of age; all the other patients had persistent seizures.

## Discussion

Using aCGH analyses, Erez et al. (2009) identified partial *CDKL5* deletions in female patients with early onset intractable epilepsy. Mei et al. (2010) identified four patients who had total or partial deletions in *CDKL5*. However, those studies included only female patients. In comparison, the aim of our study was to identify candidate

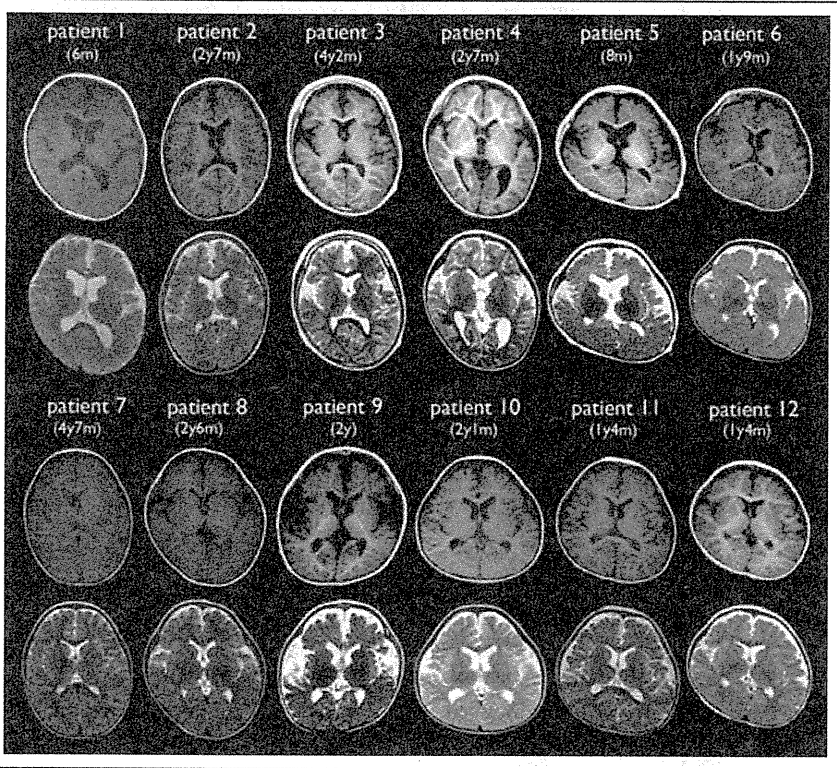


**Figure 4.**
Brain MRI findings of the patients. $T_1$- (up) and $T_2$-weighted (bottom) MRI indicates frontal atrophies in many patients, except for Patient 7. In Patient 6, spoiled gradient echo (SPGR) is shown instead of $T_1$.
*Epilepsia* © ILAE

genetic causes of early epileptic encephalopathy, and thus we recruited patients of both genders. Genomic copy numbers of whole chromosomes were comprehensively analyzed and submicroscopic chromosomal abnormalities of the *CDKL5* region were identified in both genders. The male patient (Patient 1) showed a partial deletion of *CDKL5*. Patients 2 and 3 showed large deletions in which the four neighboring genes, *CDKL5*, *RS1*, *PPEF1*, and *PHKA2*, were included. *RS1* and *PHKA2* are responsible for X-linked diseases, and the function of *PPEF1* is unknown. The remaining Patient 4 showed partial deletions of *CDKL5* and *RS1*. Therefore, phenotypic features of Patients 2, 3, and 4 suggest a causal role for *CDKL5* deletions in early epileptic encephalopathy. Despite the gender difference and the deleted size differences, the clinical severities of the patients with *CDKL5* deletions were similar between genders and similar to those of patients previously reported to have partial or total deletion of *CDKL5* (Van Esch et al., 2007; Erez et al., 2009; Bahi-Buisson et al., 2010; Mei et al., 2010).

Previously, *CDKL5* mutations were shown to affect mainly female patients, and their frequency has been estimated as approximately 9–28% in female patients with early onset seizures (Bahi-Buisson et al., 2008b; Nemos et al., 2009). However, those studies mainly included female patients. Elia et al. (2008) identified *CDKL5* mutations in three male patients with early onset epileptic encephalopathy. Male patients with *CDKL5* mutations or deletions have also been reported by others (Fichou et al., 2009; Sartori et al., 2009). In our study, initial identification of *CDKL5* deletions in both male and female patients with early epileptic encephalopathy prompted us to analyze *CDKL5* nucleotide sequences of both genders, and the results revealed nucleotide changes in two male patients and six female patients. We observed that the clinical severity of the disease did not differ between males and females. Therefore, male as well as female patients with early onset epileptic encephalopathy should be tested for *CDKL5* mutations.

Because *CDKL5* is located on Xp22.13, genetic traits of *CDKL5* alterations have been considered to be X-linked dominant, just as *MECP2* mutations are responsible for the majority of RTT cases, a neurologic disorder occurring almost exclusively in females. The rare male patients with *MECP2* mutations showed severe mental retardation but no RTT phenotype (Gomot et al., 2003). In comparison, there are no phenotypic differences between male and female patients with *CDKL5* mutations or deletions. Bahi-Buisson et al. (2008b) suggested that phenotypic heterogeneity does not correlate with the nature or the position of the mutations or with the pattern of X-chromosome inactivation. Indeed, no clear genotype–phenotype correlation between these factors has been established. Therefore, an important question is why clinical severity is the same between the genders. Based on previous reports, we know that the absence of CDKL5 protein is not lethal in males, and *CDKL5*

abnormalities result in severe neurodevelopmental delay and early onset epilepsy in both genders (Castren et al., 2011). In this study, the estimated frequencies of *CDKL5* abnormalities in patients with epileptic encephalopathy were 5% in male and 14% in female patients. Therefore, the observed difference in the frequency of *CDKL5* mutations between male and female patients may simply be a consequence of the fact that female patients have two X chromosomes.

Subjects in our study included five female patients with RTT who did not show *MECP2* mutations. However, these female patients did not carry a *CDKL5* mutation. Some researchers have found no *CDKL5* mutations in patients with RTT (Huppke et al., 2005; Li et al., 2007). Previously, *CDKL5* mutations were analyzed in patients with both classic and atypical variants of RTT. However, mutations were identified only in patients with seizure onset before 6 months of age (Evans et al., 2005; Scala et al., 2005; Artuso et al., 2010). In another study, all patients with *CDKL5* mutations showed early onset seizures that began before 6 months of age (Erez et al., 2009). These findings suggest that development of early onset seizures is an essential clinical feature in patients with *CDKL5* mutations. The onset of epileptic seizures in the first 6 months distinguishes patients with *CDKL5* mutations from patients with typical RTT caused by *MECP2* mutations (Castren et al., 2011).

All previously reported *CDKL5* mutations were sporadic and were identified as de novo. Only a small numbers of mutations were recurrent (Castren et al., 2011). In this study, we observed eight *CDKL5* mutations that included six novel and two recurrent mutations. The phenotypic features of the patients with recurrent mutations are similar to those described previously (Sartori et al., 2009; Artuso et al., 2010).

Consistent with the findings of previous studies, we observed polymorphous seizures (i.e., myoclonic seizures, tonic seizures, and spasms) in our study. The clinical course of seizure development was also identical to the proposed three stages reported by Bahi-Buisson et al. (2008a) [i.e., stage I, early onset epilepsy (onset 1–10 weeks); stage II, epileptic encephalopathy with infantile spasms and hypsarrhythmia; stage III, seizure-free in estimated 50% of patients at late infantile period] because our Patient 7 showed good seizure control after 3 years of age. Artuso et al. (2010) reported that patients with *CDKL5* mutations showed no abnormalities on brain magnetic resonance imaging (MRI). However, our findings indicated mild frontal lobe atrophy in almost all patients. Therefore, this may be an additional clinical characteristic of patients with *CDKL5* mutations.

## Acknowledgments

We thank the patients' parents for their gracious participation and support. J-S L was supported by a Research Fellowship from the Takeda Science Foundation in Japan. This research was partially supported by Research Grant from the Japan Epilepsy Research Foundation (T.Y.)

## Disclosure

None of the authors has any conflict of interest to disclose. We confirm that we have read the Journal's position on issues involved in ethical publication and affirm that this report is consistent with those guidelines.

## References

Archer HL, Evans J, Edwards S, Colley J, Newbury-Ecob R, O'Callaghan F, Huyton M, O'Regan M, Tolmie J, Sampson J, Clarke A, Osborne J. (2006) CDKL5 mutations cause infantile spasms, early onset seizures, and severe mental retardation in female patients. *J Med Genet* 43:729–734.

Artuso R, Mencarelli MA, Polli R, Sartori S, Ariani F, Pollazzon M, Marozza A, Cilio MR, Specchio N, Vigevano F, Vecchi M, Boniver C, Bernardina BD, Parmeggiani A, Buoni S, Hayek G, Mari F, Renieri A, Murgia A. (2010) Early-onset seizure variant of Rett syndrome: definition of the clinical diagnostic criteria. *Brain Dev* 32:17–24.

Bahi-Buisson N, Kaminska A, Boddaert N, Rio M, Afenjar A, Gerard M, Giuliano F, Motte J, Heron D, Morel MA, Plouin P, Richelme C, des Portes V, Dulac O, Philippe C, Chiron C, Nabbout R, Bienvenu T. (2008a) The three stages of epilepsy in patients with CDKL5 mutations. *Epilepsia* 49:1027–1037.

Bahi-Buisson N, Nectoux J, Rosas-Vargas H, Milh M, Boddaert N, Girard B, Cances C, Ville D, Afenjar A, Rio M, Heron D, N'Guyen Morel MA, Arzimanoglou A, Philippe C, Jonveaux P, Chelly J, Bienvenu T. (2008b) Key clinical features to identify girls with CDKL5 mutations. *Brain* 131:2647–2661.

Bahi-Buisson N, Girard B, Gautier A, Nectoux J, Fichou Y, Saillour Y, Poirier K, Chelly J, Bienvenu T. (2010) Epileptic encephalopathy in a girl with an interstitial deletion of Xp22 comprising promoter and exon 1 of the CDKL5 gene. *Am J Med Genet B Neuropsychiatr Genet* 153B:202–207.

Castren M, Gaily E, Tengstrom C, Lahdetie J, Archer H, Ala-Mello S. (2011) Epilepsy caused by CDKL5 mutations. *Eur J Paediatr Neurol* 15:65–69.

Elia M, Falco M, Ferri R, Spalletta A, Bottitta M, Calabrese G, Carotenuto M, Musumeci SA, Lo Giudice M, Fichera M. (2008) CDKL5 mutations in boys with severe encephalopathy and early-onset intractable epilepsy. *Neurology* 71:997–999.

Erez A, Patel AJ, Wang X, Xia Z, Bhatt SS, Craigen W, Cheung SW, Lewis RA, Fang P, Davenport SL, Stankiewicz P, Lalani SR. (2009) Alu-specific microhomology-mediated deletions in CDKL5 in females with early-onset seizure disorder. *Neurogenetics* 10:363–369.

Evans JC, Archer HL, Colley JP, Ravn K, Nielsen JB, Kerr A, Williams E, Christodoulou J, Gecz J, Jardine PE, Wright MJ, Pilz DT, Lazarou L, Cooper DN, Sampson JR, Butler R, Whatley SD, Clarke AJ. (2005) Early onset seizures and Rett-like features associated with mutations in CDKL5. *Eur J Hum Genet* 13:1113–1120.

Fichou Y, Bieth E, Bahi-Buisson N, Nectoux J, Girard B, Chelly J, Chaix Y, Bienvenu T. (2009) Re: CDKL5 mutations in boys with severe encephalopathy and early-onset intractable epilepsy. *Neurology* 73:77–78; author reply 78.

Fichou Y, Nectoux J, Bahi-Buisson N, Chelly J, Bienvenu T. (2010) An isoform of the severe encephalopathy-related CDKL5 gene, including a novel exon with extremely high sequence conservation, is specifically expressed in brain. *J Hum Genet* 56:52–57.

Gomot M, Gendrot C, Verloes A, Raynaud M, David A, Yntema HG, Dessay S, Kalscheuer V, Frints S, Couvert P, Briault S, Blesson S, Toutain A, Chelly J, Desportes V, Moraine C. (2003) MECP2 gene mutations in non-syndromic X-linked mental retardation: phenotype-genotype correlation. *Am J Med Genet A* 123A:129–139.

Huppke P, Ohlenbusch A, Brendel C, Laccone F, Gartner J. (2005) Mutation analysis of the HDAC 1, 2, 8 and CDKL5 genes in Rett syndrome patients without mutations in MECP2. *Am J Med Genet A* 137: 136–138.

Kalscheuer VM, Tao J, Donnelly A, Hollway G, Schwinger E, Kubart S, Menzel C, Hoeltzenbein M, Tommerup N, Eyre H, Harbord M, Haan E, Sutherland GR, Ropers HH, Gecz J. (2003) Disruption of the serine/threonine kinase 9 gene causes severe X-linked infantile spasms and mental retardation. *Am J Hum Genet* 72:1401–1411.

Li MR, Pan H, Bao XH, Zhang YZ, Wu XR. (2007) MECP2 and CDKL5 gene mutation analysis in Chinese patients with Rett syndrome. *J Hum Genet* 52:38–47.

Mari F, Azimonti S, Bertani I, Bolognese F, Colombo E, Caselli R, Scala E, Longo I, Grosso S, Pescucci C, Ariani F, Hayek G, Balestri P, Bergo A, Badaracco G, Zappella M, Broccoli V, Renieri A, Kilstrup-Nielsen C, Landsberger N. (2005) CDKL5 belongs to the same molecular pathway of MeCP2 and it is responsible for the early-onset seizure variant of Rett syndrome. *Hum Mol Genet* 14:1935–1946.

Mei D, Marini C, Novara F, Bernardina BD, Granata T, Fontana E, Parrini E, Ferrari AR, Murgia A, Zuffardi O, Guerrini R. (2010) Xp22.3 genomic deletions involving the CDKL5 gene in girls with early onset epileptic encephalopathy. *Epilepsia* 51:647–654.

Nabbout R, Dulac O. (2003) Epileptic encephalopathies: a brief overview. *J Clin Neurophysiol* 20:393–397.

Nabbout R, Dulac O. (2008) Epileptic syndromes in infancy and childhood. *Curr Opin Neurol* 21:161–166.

Nemos C, Lambert L, Giuliano F, Doray B, Roubertie A, Goldenberg A, Delobel B, Layet V, N'Guyen MA, Saunier A, Verneau F, Jonveaux P, Philippe C. (2009) Mutational spectrum of CDKL5 in early-onset encephalopathies: a study of a large collection of French patients and review of the literature. *Clin Genet* 76:357–371.

Pintaudi M, Baglietto MG, Gaggero R, Parodi E, Pessagno A, Marchi M, Russo S, Veneselli E. (2008) Clinical and electroencephalographic features in patients with CDKL5 mutations: two new Italian cases and review of the literature. *Epilepsy Behav* 12:326–331.

Sartori S, Di Rosa G, Polli R, Bettella E, Tricomi G, Tortorella G, Murgia A. (2009) A novel CDKL5 mutation in a 47,XXY boy with the early-onset seizure variant of Rett syndrome. *Am J Med Genet A* 149A:232–236.

Scala E, Ariani F, Mari F, Caselli R, Pescucci C, Longo I, Meloni I, Giachino D, Bruttini M, Hayek G, Zappella M, Renieri A. (2005) CDKL5/STK9 is mutated in Rett syndrome variant with infantile spasms. *J Med Genet* 42:103–107.

Shimojima K, Sugiura C, Takahashi H, Ikegami M, Takahashi Y, Ohno K, Matsuo M, Saito K, Yamamoto T. (2010) Genomic copy number variations at 17p13.3 and epileptogenesis. *Epilepsy Res* 89:303–309.

Van Esch H, Jansen A, Bauters M, Froyen G, Fryns JP. (2007) Encephalopathy and bilateral cataract in a boy with an interstitial deletion of Xp22 comprising the CDKL5 and NHS genes. *Am J Med Genet A* 143:364–369.

Zupanc ML. (2009) Clinical evaluation and diagnosis of severe epilepsy syndromes of early childhood. *J Child Neurol* 24:6S–14S.

## Supporting Information

Additional Supporting Information may be found in the online version of this article:

**Table S1.** The physical positions of BAC clones.

**Table S2.** Primer sequences for *CDKL5*.

**Table S3.** The results of aCGH.

Please note: Wiley-Blackwell is not responsible for the content or functionality of any supporting information supplied by the authors. Any queries (other than missing material) should be directed to the corresponding author for the article.

RESEARCH ARTICLE

AMERICAN JOURNAL OF medical genetics PART A

# Craniofacial and Oral Features of Sotos Syndrome: Differences in Patients With Submicroscopic Deletion and Mutation of *NSD1* Gene

**Norimitsu Hirai,[1]* Kensuke Matsune,[2] and Hirofumi Ohashi[3]**

[1]Department of Pediatric Dentistry, Nihon University Graduate School of Dentistry at Matsudo, Chiba, Japan

[2]Department of Pediatric Dentistry, Nihon University School of Dentistry at Matsudo, Chiba, Japan

[3]Division of Medical Genetics, Saitama Children's Medical Center, Saitama, Japan

Received 7 October 2010; Accepted 22 January 2011

Sotos syndrome is a well-known overgrowth syndrome caused by haploinsufficiency of *NSD1* gene located at 5q35. There are two types of mutations that cause *NSD1* haploinsufficiency: mutations within the *NSD1* gene (mutation type) and a 5q35 submicroscopic deletion encompassing the entire *NSD1* gene (deletion type). We investigated detailed craniofacial, dental, and oral findings in five patients with deletion type, and three patients with mutation type Sotos syndrome. All eight patients had a high palate, excessive tooth wear, crowding, and all but one patient had hypodontia and deep bite. Hypodontia was exclusively observed in the second premolars, and there were no differences between the deletion and mutation types in the number of missing teeth. Another feature frequently seen in common with both types was maxillary recession. Findings seen more frequently and more pronounced in deletion-type than in mutation-type included mandibular recession, scissors or posterior cross bite, and small dental arch with labioclination of the maxillary central incisors. It is noteworthy that although either scissors bite or cross bite was present in all of the deletion-type patients, neither of these was observed in mutation-type patients. Other features seen in a few patients include enamel hypoplasia (two deletion patients), and ectopic tooth eruption (one deletion and one mutation patients). Our study suggests that Sotos syndrome patients should be observed closely for possible dental and oral complications especially for malocclusion in the deletion-type patients. 

**Key words:** Sotos syndrome; *NSD1*; submicroscopic deletion; small dental arch; malocclusion; mandibular recession

**How to Cite this Article:**
Hirai N, Matsune K, Ohashi H. 2011. Craniofacial and oral features of Sotos syndrome: differences in patients with submicroscopic deletion and mutation of *NSD1* gene.
Am J Med Genet Part A 155:2933–2939.

## INTRODUCTION

Sotos syndrome is a congenital genetic disorder characterized by overgrowth starting before birth, specific facial manifestations (macrocephaly, prominent forehead, hypertelorism, downslanting palpebral fissures, and pointed chin), advanced bone age, and developmental impairment. Since its initial description by Sotos et al. [1964] several hundred patients have been reported to date. It may be accompanied by a variety of complications, including cardiovascular, urinogenital, and ophthalmic malformations, skeletal abnormalities, and seizures. Dental and oral findings have been reported to include premature tooth eruption, hypodontia, enamel hypoplasia, excessive tooth wear, maxillary and mandibular recession, talon cusps, fused teeth, and expanded pulp cavity of deciduous teeth [Welbury and Fletcher, 1988; Cole and Hughes, 1994; Inokuchi et al., 2001; Gomes-Silva et al., 2006; Takei et al., 2007; Nishimura et al., 2008].

Kurotaki et al. [2002] reported that this syndrome is caused by haploinsufficiency of the *NSD1* nuclear receptor SET domain containing protein 1 gene located on 5q35. There are two main types that cause *NSD1* haploinsufficiency: mutations within the *NSD1* gene, and a submicroscopic deletion in the region that contains the *NSD1* gene (constant deletion of approximately 2.2 Mb including *NSD1* and around 20 neighboring genes) [Kurotaki et al., 2002]. Nagai et al. [2003] investigated differences in clinical manifestations between these two types, and reported

Grant sponsor: Ministry of Education, Culture, Sports, Science and Technology (MEXT); Grant number: 2008-2012; Grant sponsor: Ministry of Health, Labour and Welfare, Japan.
*Correspondence to:
Norimitsu Hirai, Department of Pediatric Dentistry, Nihon University Graduate School of Dentistry at Matsudo, 2-870-1 Sakaecho-Nishi, Matsudo, Chiba 271-8587, Japan. E-mail: hirai.norimitsu@nihon-u.ac.jp
Published online 19 October 2011 in Wiley Online Library (wileyonlinelibrary.com).
DOI 10.1002/ajmg.a.33969

that major anomalies such as central nervous, cardiovascular, and urinogenital abnormalities are more common in the deletion-type. Their only reference to dental findings, however, stated that early tooth eruption occurred in both types with no significant difference.

The first detailed investigation of dental and oral findings seen in Sotos syndrome based on *NSD1* genetic diagnosis was carried out by Kotilainen et al. [2009]. They analyzed dental and oral findings from 13 patients with Sotos syndrome (all except one with the mutation type), including panoramic imaging, and reported the characteristic oral complications of Sotos syndrome, including hypodontia of the second premolars. We here report on the results of our investigation of detailed craniofacial, dental, and oral findings in five patients with deletion-type, and three patients with mutation-type Sotos syndrome.

## MATERIALS AND METHODS

### Patients

The eight patients comprised a group who underwent examination at Saitama Children's Medical Center. Five patients (three males, two females; age, 6–13 years) were identified as having a submicroscopic deletion on 5q35 including the *NSD1* gene, and three (all females; age, 6–10 years) were identified as having a mutation of the *NSD1* gene. Deletions were identified by fluorescence in situ hybridization (FISH) analysis of metaphase chromosomes from peripheral blood, using a total of seven bacterial artificial chromosome (BAC) clones comprising the BAC clone that includes the *NSD1* gene (RP11-99N22) together with those toward the centromere (RP11-880A16, RP11-690I8, RP11-991B23) and toward the telomere (RP11-147K7, RP11-452O4, and RP11-158F10). The results showed that the same ~2 Mb deletion was present in all five patients. Mutation analysis using genomic DNA extracted from peripheral blood was performed by polymerase chain reaction (PCR) and direct sequencing of all translated regions for exon 2–23. The results identified mutations generating premature termination in both Patients 6 and 7, comprising a five base deletion (2053–2057delAAGTA) and a base deletion (5431delC), respectively, and a missense mutation (4991G>C) in Patient 8. Details of clinical manifestations are shown in Table I. This study protocol was approved by the Ethics Committee of Saitama Children's Medical Center and proper informed consents were obtained from the legal guardians of the patients.

### Oral and Dental Studies

Physical examination and dental cast studies were used to evaluate palatal morphology, tooth calcification, dental arches, occlusion, tooth size, and tooth eruption status. Panoramic and lateral cephalometric radiographs reconstructed from multi-detector row computed tomography (MDCT) were also used to evaluate the relationship of craniofacial, dental and skeletal structures, and hypodontia [Hirai et al., 2010; Yamauchi et al., 2010]. Crown and

TABLE I. Clinical Manifestations of Eight Patients With Sotos Syndrome

| | Deletion type patients | | | | | Mutation type patients | | |
|---|---|---|---|---|---|---|---|---|
| | 1 | 2 | 3 | 4 | 5 | 6 | 7 | 8 |
| Gender | M | F | F | M | M | F | F | F |
| Ages (years) | 7 | 8 | 6 | 7 | 13 | 7 | 10 | 6 |
| Overgrowth | – | – | – | – | – | + | + | + |
| Intellectual disability | Moderate | Moderate | Moderate | Moderate | Moderate | Mild | – | Mild |
| Seizure | – | + | – | + | – | – | + | – |
| Craniofacial features | | | | | | | | |
| Macrocephaly | + | + | + | – | + | + | + | – |
| Prominent forehead | + | + | + | + | + | + | + | – |
| Hypertelorism | + | + | + | + | + | + | + | + |
| Downslanting palpebral fissures | + | + | + | + | + | + | + | + |
| Pointed chin | + | + | + | + | + | + | + | + |
| Strabismus | + | + | + | – | – | + | – | – |
| Skeletal anomaly | | | | | | | | |
| Scoliosis | – | – | – | + | + | – | + | + |
| Pes planovalgus | + | + | + | + | + | + | – | + |
| Cardiovascular anomaly | AR | PDA | – | PDA, ASD, VSD | – | VSD, CoA | MR | – |
| Urogenital anomaly | Hydronephrosis, VUR | – | – | – | – | Urethrocele | Hydronephrosis, hydroureter | – |
| Others | Hearing loss | Myelomeningocele, umblical hernia | – | – | – | – | – | – |

M, male; F, female; AR, aortic regurgitation; PDA, patent ductus arteriosus; ASD, atrial septal defect; VSD, ventricular septal defect, CoA, coarctation of aorta; MR, mitral regurgitation; VUR, vesicoureteral reflux; +, present; –, absent.

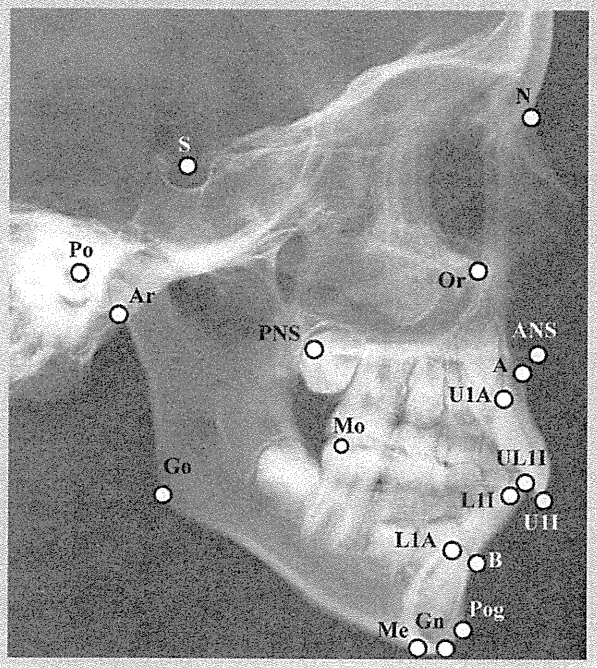


FIG. 1. Landmark points, angles, and lines used in cephalometoric analysis and profilogram. Landmarks: N, nasion; Or, orbitale; S, sella turcia; Po, porion; Ar, articulare; Go, gonion; Me, menton; Gn, gnathion; Pog, pogonion; A, A-point; B, B-point; ANS, anterior nasal spine; Mo, molar occlusion; U1A, upper central incisor root apex; U1I, upper central incisor edge; L1A, lower central incisor root apex; L1I, lower central incisor edge; UL1I, middle of U1I and L1I. Angles: convexity, N-A line to the A-Pog line; A-B plane, N-Pog line to the A-B line; SNA, S-N line to the N-A line; SNB, S-N line to the N-B line; facial angle, Po-Or line to the N-Pog line; SNP, S-N line to the N-Pog line; *y*-axis, Po-Or line to the S-Gn line; SN-S·Gn, S-N line to the S-Gn line; mandibular plane, Po-Or line to the Me-the lower border of the mandible line; gonial angle, Ar-the posterior border of the ramus of the mandible line to the Me-the lower border of the mandible line; GZN, S-N line to the Ar-the posterior border of the ramus of the mandible line; FH to SN, Po-or line to the S-N line; U-1 to FH plane, U1I-U1A line to the Po-or line; U-1 to SN plane, U1I-U1A line to the S-N line; L-1 to mandibular, L1I-L1A line to the Me-the lower border of the mandible; interincisal, U1I-U1A line to the L1I-L1A line; occlusal plane, Po-Or line to the Mo-UL1I line.

dental arch sizes were measured using a caliper with a resolution accuracy of 0.01 mm. Lateral cephalometric analysis was performed based on the method developed by Iizuka and Ishikawa [1957] (Fig. 1). All data in this study (tooth size, dental arch form size, and cephalometric findings) were compared with standard values for Japanese individuals [Otsubo, 1957; Otsubo et al., 1964].

## RESULTS

Oral and dental anomalies noted in eight patients are summarized in Table II. All eight patients had a high palate, crowding, and excessive tooth wear. All but one (Patient 1 with *NSD1* deletion) had hypodontia exclusively in the second premolars. There were no differences between the deletion-type and mutation-types in the number of missing teeth (mean number of missing teeth was 2 in the deletion-type and 2.6 in the mutation-type) (Fig. 2). The results of cephalometric analysis showed that among the five deletion-type patients, maxillary and mandibular recession was present in three and maxillary recession alone in one, whereas among the three mutation-type patients maxillary and mandibular recession was present in one and maxillary recession alone in one. The deletion-type was regarded as having a stronger tendency for mandibular recession (Table III). In terms of occlusion, crowding was present in all patients, and deep bite was seen in all but one (Patient 2 with *NSD1* deletion). It is noteworthy that although either scissors bite (Patients 1, 3, and 4) or cross bite (Patients 2 and 5) was present in all of the deletion-type patients, neither of these was observed in mutation-type patients (Fig. 3).

Small dental arch was present in all the deletion-type patients and one mutation-type patient (Table IV). In terms of morphological categories of small dental arch, the maxilla exhibited a narrow dental arch with labioclination of the central incisors in all five deletion-type patients, with the mandible being saddle-shaped in three patients and U-shaped in two, while the mutation-type patient had U-shaped upper and lower dental arches (Fig. 4). In terms of tooth size, both microdontia and macrodontia were occasionally seen in both the deletion-type and mutation-types, but no characteristic findings were present in either type (data not shown). Enamel hypoplasia was present in two out of the five deletion-type patients (Patients 2 and 3), but was not present in the mutation-type. In addition, ectopic eruption of the first molar was present in one deletion-type patient (Patient 4, right mandibular) and one mutation-type patient (Patient 6, bilateral maxillary). Some representative photographs of oral and dental anomalies noted in patients studied are shown in Figure 5.

## DISCUSSION

The oral manifestations observed in common with both deletion and mutation type Sotos syndrome patients noted here were a high palate, excessive tooth wear, recession of maxilla, deep bite, crowding, and hypodontia. Hypodontia has been previously described by several authors [Inokuchi et al., 2001; Callnan et al., 2006; Gomes-Silva et al., 2006; Nishimura et al., 2008]. Kotilainen et al. [2009] recently investigated 13 patients with Sotos syndrome (12 patients with *NSD1* mutations and one with *NSD1* deletion) and found one or more premolar teeth were absent in 9 out of 13 patients (8 out of 12 mutation patients and one deletion-type patient). Based on the observation that the deletion patient had the most severe phenotype of tooth agenesis, involving not only the second premolars and the third molars, but also one mandibular incisor, they noted the possibility that patient with the *NSD1* deletion had the most severe tooth agenesis. In our study, however, which included five deletion-type patients, although similar high rates of hypodontia were observed in both the deletion-type and mutation-type, we did not observe any difference in severity in either the deletion-type or mutation-type.

One noteworthy difference between the deletion-type and mutation-type was the fact that either scissors bite or cross bite

TABLE II. Oral and Dental Anomalies in Eight Patients

| | Deletion type patients | | | | | Mutation type patients | | | Total | |
|---|---|---|---|---|---|---|---|---|---|---|
| **Oral anomalies** | **1** | **2** | **3** | **4** | **5** | **6** | **7** | **8** | **Deletion type** | **Mutation type** |
| High palate | + | + | + | + | + | + | + | + | 5/5 | 3/3 |
| Excessive tooth wear | + | + | + | + | + | + | + | + | 5/5 | 3/3 |
| Hypodontia | − | + | + | + | + | + | + | + | 4/5 | 3/3 |
| Maxillary recession | + | − | + | + | + | + | + | − | 4/5 | 2/3 |
| Mandibular recession | − | − | + | + | + | − | + | − | 3/5 | 1/3 |
| Malocclusion | | | | | | | | | | |
| Scissors bite | + | − | + | + | − | − | − | − | 3/5 | 0/3 |
| Cross bite | − | + | − | − | + | − | − | − | 2/5 | 0/3 |
| Deep bite | + | − | + | + | + | + | + | + | 4/5 | 3/3 |
| Crowding | + | + | + | + | + | + | + | + | 5/5 | 3/3 |
| Small dental arch | + | + | + | + | + | − | + | − | 5/5 | 1/3 |
| Maxilla | N | N | N | N | N | U | U | U | | |
| Mandibula | S | U | S | S | U | U | U | U | | |
| Labioclination of maxillary central incisor | + | + | + | + | + | − | − | − | 5/5 | 0/3 |
| Enamel hypoplasia | − | + | + | − | − | − | − | − | 2/5 | 0/3 |
| Ectopic tooth eruption | − | − | − | + | − | + | − | − | 1/5 | 1/3 |

N, narrow dental arch; U, U-shaped dental arch; S, saddle-shaped dental arch; +, present; −, absent.

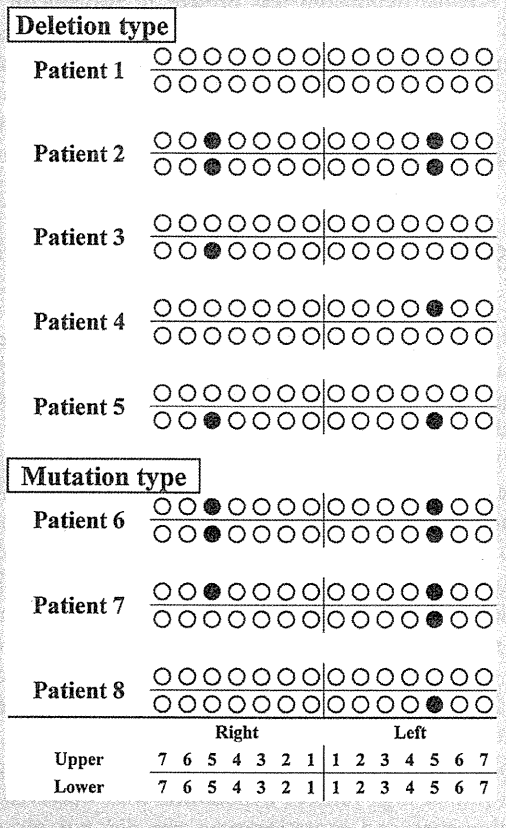


FIG. 2. Hypodontia in eight patients with Sotos syndrome. ●, Congenitally missing teeth.

was observed in all deletion-type patients, whereas neither was present in the mutation-type. All of the deletion-type patients had small dental arches, and in terms of morphological categories, the maxilla exhibited a narrow dental arch with labioclination of the central incisors in all five deletion-type patients, with the mandible being saddle-shaped in three patients and U-shaped in two. Only one single mutation-type patient had small dental arches with both upper and lower dental arches being U-shaped. Narrowing of the dental arch is more pronounced in the narrow-shape and saddle-shape compared with the U-shape. It is possible that the degree of narrowing of the dental arch in the deletion-type and the misalignment in arch morphology between the maxilla and mandible causes scissors bite or cross bite.

In addition, maxillary and mandibular recession has also been reported as a dental manifestation of Sotos syndrome [Welbury and Fletcher, 1988; Takei et al., 2007]. In our results, there was a tendency toward maxillary and mandibular recession in the deletion-type and maxillary recession in the mutation-type. Based on these findings, there was a tendency for maxillary recession to occur in both the deletion-type and mutation-type, but there was also a tendency toward the occurrence of mandibular recession in the deletion-type. Taken in conjunction with the pronounced mandibular recession seen in the deletion-type on cephalometric analysis, mandibular malformations, including those of the dental arch, may be regarded as characteristic of the deletion-type. The cause is unknown, but in the deletion-type, minute genome imbalances, involving considerable number of genes other than the *NSD1* gene, may either: (1) directly cause deficient growth of the mandibular area; or (2) secondarily cause malocclusion or abnormal dental arch morphology as a result of dysfunction of the perioral muscles associated with more

TABLE III. Lateral Cephalometric Analysis With MDCT of Eight Patients

| | Deletion type patients | | | | | Mutation type patients | | |
|---|---|---|---|---|---|---|---|---|
| | 1 | 2 | 3 | 4 | 5 | 6 | 7 | 8 |
| Skeletal | | | | | | | | |
| Covexity | −2.56 | −1.05 | −0.66 | −1.80 | −1.95 | −4.56 | −2.52 | −2.94 |
| A–B plane | −1.12 | −3.96 | 1.68 | −0.32 | 1.40 | 2.15 | 1.96 | 2.56 |
| SNA | −2.54 | 1.24 | −2.28 | −3.45 | −2.32 | −2.69 | −3.18 | −1.63 |
| SNB | −1.80 | 1.71 | −3.31 | −3.18 | −2.84 | −0.76 | −2.29 | −0.07 |
| Facial angle | 0.68 | −3.23 | −0.47 | 0.38 | 0.34 | 0.38 | −1.55 | 1.43 |
| SNP | −0.71 | 1.77 | −1.76 | −1.16 | −0.63 | 0.02 | −2.22 | 0.11 |
| *Y*-axis | −0.50 | −0.37 | −0.38 | −0.08 | 0.17 | −0.36 | 1.29 | −1.34 |
| SN-S-Gn | 3.08 | −1.30 | 0.32 | 3.86 | 0.93 | 0.22 | 1.86 | −0.30 |
| Mandibular plane | 1.29 | 1.05 | −1.47 | 0.30 | 1.12 | −0.58 | 1.98 | −0.29 |
| Gonial angle | 6.24 | −0.15 | −4.06 | −5.27 | 0.73 | 0.29 | 0.44 | 3.06 |
| GZN | 0.77 | 0.09 | 3.01 | 2.84 | 1.19 | −0.37 | 1.52 | −0.27 |
| FH to SN | 2.38 | −1.15 | 0.71 | 2.55 | 0.98 | 0.52 | 0.97 | 1.37 |
| Denture | | | | | | | | |
| U-1 to FH plane | 1.30 | 1.37 | 2.94 | 0.30 | 0.72 | −0.47 | 0.50 | 0.69 |
| U-1 to SN plane | 0.51 | 1.87 | 2.56 | −0.52 | 0.24 | −0.64 | −0.46 | 0.21 |
| L-1 to mandibular | −2.24 | −0.47 | 0.98 | −1.47 | −1.64 | −2.39 | −0.46 | −1.93 |
| Interincisal | −0.07 | −1.07 | −1.53 | 0.46 | 0.22 | 1.90 | −0.83 | 0.71 |
| Occlusal plane | −0.99 | 1.09 | −0.76 | −0.24 | 2.97 | −1.37 | 1.35 | −0.49 |

Unit, SD.

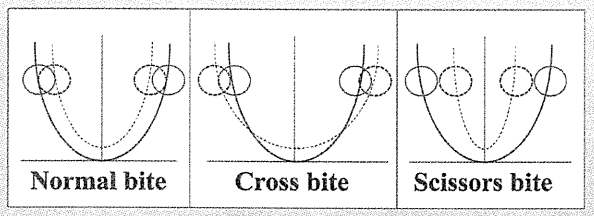


**FIG. 3. Schematic representations of normal and abnormal occlusions. ————, Maxillary dental arch; - - - - - - -, mandibular dental arch; ◯, maxillary first molar; ◯, mandibular first molar.**

pronounced developmental impairment [Grabowski et al., 2007a,b; Stahl et al., 2007].

Enamel hypoplasia has also been reported as a dental manifestation of Sotos syndrome [Inokuchi et al., 2001]. Kotilainen et al. [2009] reported enamel hypoplasia in four out of 13 patients (all mutation type). In our study, enamel hypoplasia was present in two out of five deletion-type patients, but not in any mutation-type patients. Enamel hypoplasia is thought to be a common manifestation that can occasionally occur in both the deletion-type and mutation-type rather than a manifestation that is prone to occur in either type.

As mild to moderate intellectual disability is common in Sotos syndrome, conventional panoramic, and cephalometric studies

TABLE IV. Dental Arch Measurements in Eight Patients

| | Deletion type patients | | | | | Mutation type patients | | |
|---|---|---|---|---|---|---|---|---|
| | 1 | 2 | 3 | 4 | 5 | 6 | 7 | 8 |
| Maxillary | | | | | | | | |
| $W_c$ | −0.55 | Deciduous | 0.04 | Deciduous | 1.79 | −1.75 | 0.61 | −1.30 |
| $W_6$ | −3.76 | −3.59 | 0.02 | −4.18 | −3.11 | −1.73 | −2.04 | −1.76 |
| $L_{16}$ | 2.68 | 1.33 | 2.88 | 1.02 | −0.69 | 1.44 | 0.14 | −1.36 |
| Mandibular | | | | | | | | |
| $W_c$ | Deciduous | Deciduous | −1.00 | Deciduous | −0.73 | −1.81 | −2.70 | −0.30 |
| $W_6$ | −4.82 | −2.51 | −2.16 | −4.45 | −3.38 | −1.57 | −4.34 | 0.96 |
| $L_{16}$ | 0.81 | 1.32 | 1.85 | 0.63 | −3.40 | 0.20 | −2.07 | 0.56 |

Unit, SD.
The $W_c$ and $W_6$ represent the distance between the primary cuspids (the cuspids), and the first molars, respectively. The $L_{16}$ represents the length from the mesial surface of the first molars to central point of incisors.

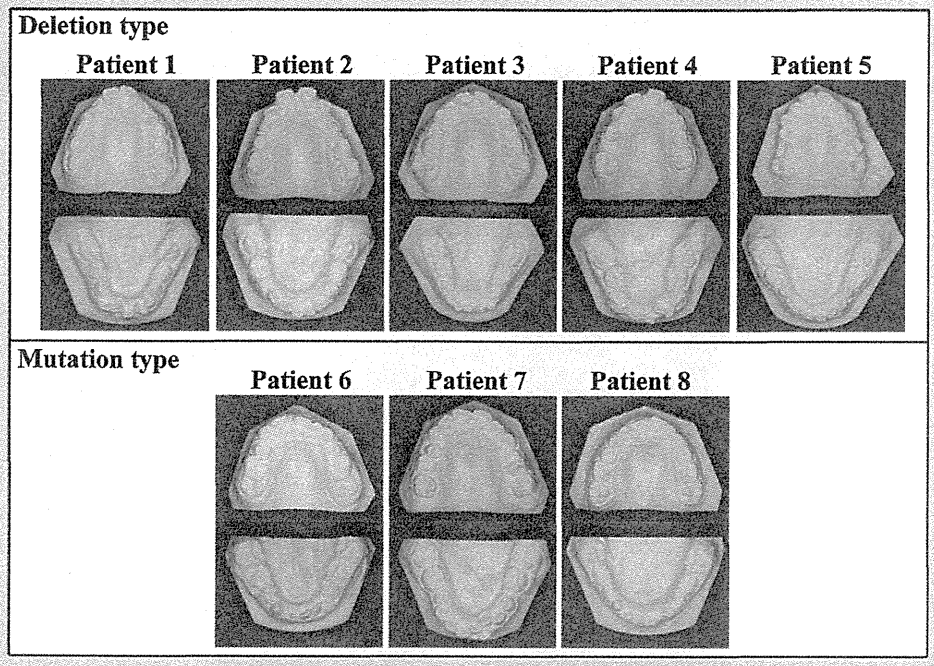


FIG. 4. Dental arch shapes of eight patients. Upper panel: maxillary dental casts, lower panel: mandibular dental casts. A narrow maxillary dental arch with labioclination of the central incisors is noted in all five deletion type patients, with the mandibula being saddle-shaped in three patients (Patients 1, 3, and 4) and U-shaped in two (Patients 2 and 5), while U-shaped upper and lower dental arches are noted in all three mutation-type patients (Patients 6, 7, and 8).

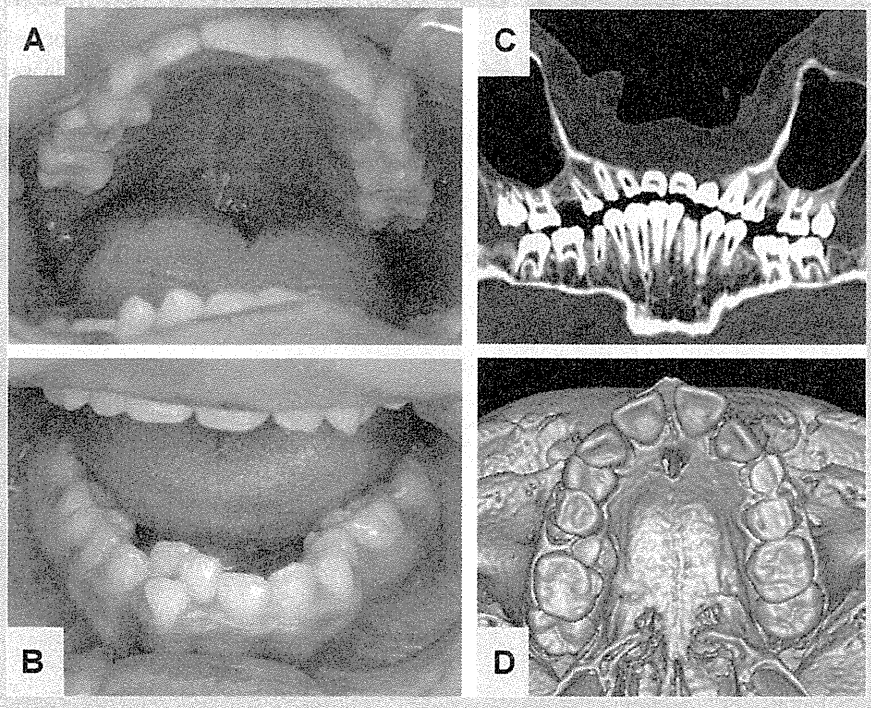


FIG. 5. Oral photographs (A,B) and MDCT-synthesized panoramic radiograph (C) of Patient 7 at age of 10 years and MDCT-synthesized upper dental arch of Patient 6 at age of 7 years (D). Note: high palate, malocclusion, small dental arch, excessive tooth wear (A,B), missing upper second premolars on both side and lower left second premolar (C), ectopic tooth eruption of first molars on both side (D).

were often difficult to perform in childhood. Thus, in this study, MDCT was used as a substitute for cephalometric radiographs and panoramic radiographs, and by which maxillofacial manifestations could be accurately evaluated [Hirai et al., 2010; Yamauchi et al., 2010].

In view of oral and dental management, we would like to provide recommendations as follows: periodic dental check up to prevent dental caries or gingivitis should be started early after one or more deciduous teeth have erupted. Around age 7 years, detailed oral and dental evaluations, including dental cast studies and MDCT, is recommended for possible hypodontia and malocclusion. If the patient has hypodontia, preceding deciduous tooth (teeth) should be maintained as long as possible with proper care. Although malocclusion like scissors bite and cross bite requires early treatment, including expansion of upper or lower jaw, to prevent craniofacial disabilities such as facial asymmetry and temporomandibular joint dysfunction, the treatment should be carefully decided based on consideration of capability of cooperation of the patients.

In conclusion, features seen more frequently and more pronounced form in deletion-type than in mutation-type were small dental arch with labioclination of the maxillary central incisors, mandibular recession, and scissors or posterior cross bite. Sotos syndrome patients should be followed closely for possible dental and oral complications especially for malocculusion in the deletion-type.

## ACKNOWLEDGMENTS

The authors are grateful to Prof. Takahide Maeda for his helpful advice. We also thank to Dr. Kenji Shimizu, Dr. Yasuo Takahashi, and Hitoshi Yabe for their invaluable assistance. This study was funded in part by a Grant for the Support of Projects for Strategic Research at Private Universities by the Ministry of Education, Culture, Sports, Science and Technology (MEXT; 2008-2012), and by a grant from the Ministry of Health, Labour and Welfare, Japan.

## REFERENCES

Callnan AP, Anand P, Sheehy EC. 2006. Sotos syndrome with hypodontia. Inter J Paediatri Dent 16:143–146.

Cole TRP, Hughes HE. 1994. Sotos syndrome: A study of the diagnostic criteria and natural history. J Med Genet 31:20–32.

Gomes-Silva JM, Ruviere DB, Segatto RA, de Queiroz AM, de Freitas AC. 2006. Sotos syndrome: A case report. Spec Care Dentist 26:257–262.

Grabowski R, Kundt G, Stahl F. 2007a. Interrelation between occlusal findings and orofacial myofunctional status in primary and mixed dentition: Part III: Interrelation between malocclusions and orofacial dysfunctions. J Orofac Orthop 68:462–476.

Grabowski R, Stahl F, Gaebel M, Kundt G. 2007b. Relationship between occlusal findings and orofacial myofunctional status in primary and mixed dentition. Part I: Prevalence of malocclusions. J Orofac Orthop 68:26–37.

Hirai N, Yamauchi T, Matsune K, Kobayashi R, Yabe H, Ohashi H, Maeda T. 2010. A comparison between two dimensional and three dimensional cephalometry on lateral radiographs and multi detector row computed tomography scans of human skulls. Int J Oral-Med Sci 9:101–107.

Iizuka T, Ishikawa F. 1957. Normal standards for various cephalometric analysis in Japanese adults. Nippon Kyosei Shika Gakkai Zasshi 16:4–12.

Inokuchi M, Nomura J, Mtsumura Y, Sekida M, Tagawa T. 2001. Sotos syndrome with enamel hypoplasia: A case report. J Clin Pediatr Dent 25:313–316.

Kotilainen J, Pohjola P, Pirinen S, Arte S, Nieminen P. 2009. Premolar hypodontia is a common feature in Sotos syndrome with a mutation in the NSD1 gene. Am J Med Genet Part A 149A:2409–2414.

Kurotaki N, Imaizumi K, Harada N, Masuno M, Kondoh T, Nagai T, Ohashi H, Naritomi K, Tsukahara M, Makita Y, Sugimoto T, Sonoda T, Hasegawa T, Chinen Y, Tomita HH, Kinoshita A, Yoshiura KK, Ohta T, Kishino T, Fukushima Y, Niikawa N, Matsumoto N. 2002. Haploinsufficiency of NSD1 causes Sotos syndrome. Nat Genet 30:365–366.

Nagai T, Matsumoto N, Kurotaki N, Harada N, Niikawa N, Ogata T, Imaizumi K, Kurosawa K, Kondoh T, Ohashi H, Tsukahara M, Makita Y, Sugimoto T, Sonoda T, Yokoyama T, Uetake K, Sakazume S, Fukushima Y, Naritomi K. 2003. Sotos syndrome and haploinsufficiency of NSD1: Clinical features of intragenic mutations and sub microscopic deletions. J Med Genet 40:285–289.

Nishimura K, Mori Y, Yamauchi M, Kamakura N, Homma H, Namura H, Miyamoto E, Matsumoto M, Shintani S, Ooshima T. 2008. Sotos syndrome with oligodontia: A case report. Pediatric Dent J 18:187–191.

Otsubo J. 1957. A study on the tooth material in Japanese adults of normal occlusion, its relationship to coronal and basal arches. Nippon Kyosei Shika Gakkai Zasshi 16:36–46.

Otsubo J, Ishikawa F, Kuwahara Y. 1964. A longitudinal study of dental development between 6–13 years of age: Growth changes of dentition. Nippon Kyosei Shika Gakkai Zasshi 23:182–190.

Sotos JF, Dodge PR, Muirhead Dl, Crawford JD, Talbot NB. 1964. Cerebral gigantism in childhood. A syndrome of excessively rapid growth with acromegatic features and a nonprogressive neurologic disorder. N Engl J Med 271:109–116.

Stahl F, Grabowski R, Gaebel M, Kundt G. 2007. Relationship between occlusal findings and orofacial myofunctional status in primary and mixed dentition. Part II: Prevalence of orofacial dysfunctions. J Orofac Orthop 68:74–90.

Takei K, Sueishi K, Yamaguchi H, Ohtawa Y. 2007. Dentofacial growth in patients with Sotos syndrome. Bull Tokyo Dent Coll 48:73–85.

Welbury RR, Fletcher HJ. 1988. Cerebral gigantism (Sotos syndrome) two case reports. J Paediatr Dent 4:41–44.

Yamauchi T, Hirai N, Matsune K, Kobayashi R, Yabe H, Ohashi H, Maeda T. 2010. Accuracy of tooth development stage, tooth size and dental arch width in multi detector row computed tomography scans of human skulls. Int J Oral Med Sci 9:108–114.

DNA Repair 10 (2011) 314–321

Contents lists available at ScienceDirect

DNA Repair

journal homepage: www.elsevier.com/locate/dnarepair

# Two unrelated patients with *MRE11A* mutations and Nijmegen breakage syndrome-like severe microcephaly

Yoshiyuki Matsumoto[a], Tatsuo Miyamoto[a], Hiromi Sakamoto[a], Hideki Izumi[a], Yuka Nakazawa[b], Tomoo Ogi[b], Hidetoshi Tahara[c], Shozo Oku[d], Azuma Hiramoto[e], Toshihide Shiiki[f], Yoshiki Fujisawa[g], Hirofumi Ohashi[h], Yoshihiro Sakemi[i], Shinya Matsuura[a,*]

[a] *Department of Genetics and Cell Biology, Research Institute for Radiation Biology and Medicine, Hiroshima University, Kasumi 1-2-3, Minami-ku, Hiroshima 734-8553, Japan*
[b] *Department of Molecular Medicine, Atomic Bomb Disease Institute, Nagasaki University, Sakamoto 1-12-4, Nagasaki 852-8523, Japan*
[c] *Department of Cellular and Molecular Biology, Graduate School of Biomedical Sciences, Hiroshima University, Kasumi 1-2-3, Minami-ku, Hiroshima 734-8553, Japan*
[d] *Kagoshima Kodomo Hospital, Ijuin-cho 2-2000-669, Hioki 899-2503, Japan*
[e] *Hokkaido Ryoikuen, Shunkoudai 4-10, Asahikawa 071-8144, Japan*
[f] *Tobu Ryoiku Center, Shinsuna 3-3-25, Koutou-ku 136-0075, Tokyo, Japan*
[g] *Ehime Prefectural Central Hospital, Kasugamachi 83, Matsuyama 790-0024, Japan*
[h] *Saitama Children's Medical Center, Iwatsuki-ku, Saitama 339-8551, Japan*
[i] *Beppu Medical Center, Uchikamado, Beppu 874-0011, Japan*

ARTICLE INFO

*Article history:*
Received 19 August 2010
Received in revised form
25 November 2010
Accepted 10 December 2010
Available online 12 January 2011

*Keywords:*
Nijmegen breakage syndrome (NBS)
Ataxia–telangiectasia-like disorder (ATLD)
Nijmegen breakage syndrome-like disorder (NBSLD)
ATM
MRE11
NBS1
Microcephaly

ABSTRACT

MRE11 and NBS1 function together as components of a MRE11/RAD50/NBS1 protein complex, however deficiency of either protein does not result in the same clinical features. Mutations in the *NBN* gene underlie Nijmegen breakage syndrome (NBS), a chromosomal instability syndrome characterized by microcephaly, bird-like faces, growth and mental retardation, and cellular radiosensitivity. Additionally, mutations in the *MRE11A* gene are known to lead to an ataxia–telangiectasia-like disorder (ATLD), a late-onset, slowly progressive variant of ataxia–telangiectasia without microcephaly. Here we describe two unrelated patients with NBS-like severe microcephaly (head circumference −10.2 SD and −12.8 SD) and mutations in the *MRE11A* gene. Both patients were compound heterozygotes for a truncating or missense mutation and carried a translationally silent mutation. The truncating and missense mutations were assumed to be functionally debilitating. The translationally silent mutation common to both patients had an effect on splicing efficiency resulting in reduced but normal MRE11 protein. Their levels of radiation-induced activation of ATM were higher than those in ATLD cells.



## 1. Introduction

The development of the central nervous system is highly sensitive to DNA damaging agents and therefore several autosomal recessive disorders with defective DNA damage repair exhibit neurological abnormalities such as microcephaly and neurodegeneration [1,2].

The MRE11/RAD50/NBS1 (MRN) protein complex and the ataxia–telangiectasia mutated (ATM) protein, together play a central role in DNA double strand break repair [3]. Mutations in the *ATM* (MIM# 607585) and *MRE11A* (MIM# 600814) genes each give rise to a progressive cerebellar ataxia syndrome: *ATM* mutations to ataxia–telangiectasia (A–T [MIM# 208900]) [4], and *MRE11A* mutations to ataxia–telangiectasia-like disorder (ATLD [MIM# 604391]) [5,6]. A–T is an autosomal recessive disorder characterized by growth deficiency, progressive cerebellar ataxia, dysarthria, telangiectasia, frequent respiratory infections, and immunodeficiency. ATLD is also characterized by cerebellar ataxia, but its onset is later in life and its progression is slower than in A–T. In addition, there is no telangiectasia and immunoglobulin levels are normal.

Mutations in two different genes involved in the MRE11/RAD50/NBS1 complex are known to lead to a hereditary disorder with severe microcephaly: the *NBN* gene (MIM# 602667) to Nijmegen breakage syndrome (NBS [MIM# 251260]) [7–9], and the *RAD50* gene (MIM# 604040) to Nijmegen breakage syndrome-like disorder (NBSLD [MIM# 613078]) [10]. NBS is an autosomal recessive disorder characterized by microcephaly, growth and mental retardation, immunodeficiency, radiosensitivity, and cancer predisposition; NBSLD is a disorder with microcephaly, mental retardation, bird-like face, and short stature,

* Corresponding author. Tel.: +81 82 257 5809; fax: +81 82 256 7101.
*E-mail address:* shinya@hiroshima-u.ac.jp (S. Matsuura).

1568-7864/$ – see front matter © 2010 Elsevier B.V. All rights reserved.
doi:10.1016/j.dnarep.2010.12.002

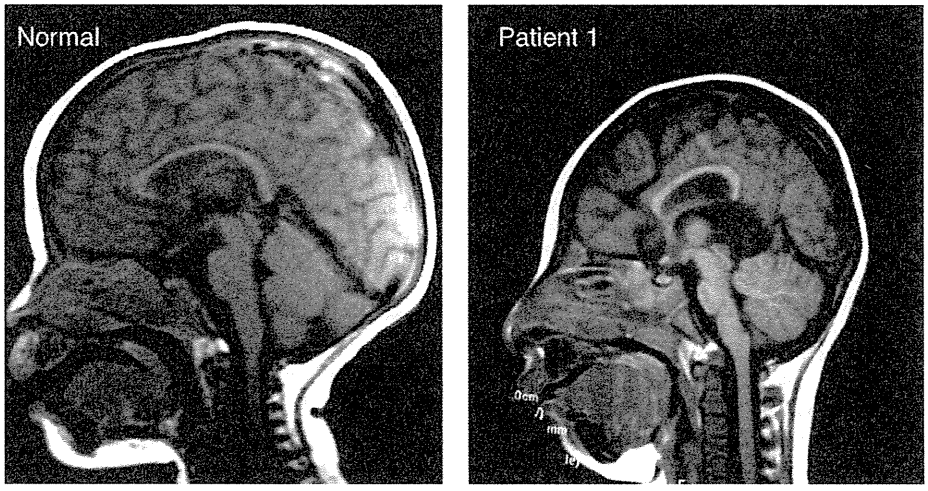


**Fig. 1.** Sagittal brain magnetic resonance imaging. (Left) Normal individual. (Right) Patient 1 at age 18 months with generalized cerebral hypodysplasia.

but without severe infections, immunodeficiency, or cancer predisposition.

We here describe two unrelated patients with Nijmegen breakage syndrome-like severe microcephaly and compound heterozygous mutations in the *MRE11A* gene.

## 2. Materials and methods

### 2.1. Clinical report

A 35-year-old woman was referred to us at 18 weeks of pregnancy for evaluation of intrauterine growth retardation. Ultrasound scan showed a fetus with a small femora and a disproportionately small head. Caesarian section was performed at 32 weeks of pregnancy, and a boy (Patient 1), was delivered. His birth weight was 966 g (−4.8 SD), length 35 cm (−6.7 SD), and head circumference 22 cm (−8.1 SD). He had severe microcephaly, a bird-headed facial appearance with receding forehead, and a prominent nose. Anterior fontanel was not palpable. His parents and two elder brothers were all healthy and phenotypically normal. There was no family history of consanguinity. Brain magnetic resonance imaging at age 18 months demonstrated hypoplasia of the cerebrum, smooth gyri, and enlarged lateral ventricles (Fig. 1). He had patent ductus arteriosus, which was surgically corrected at age 5 months. Bilateral cryptochidism was operated on at age 3 years. He stood holding onto a chair at age 30 months, sat alone with a stoop at age 3 years, and walked at age 3 years. At age 3.5 years, he weighed 7.4 kg (−4.1 SD), measured 78.5 cm (−4.8 SD), and had a head circumference of 34 cm (−10.2 SD). G-banded chromosomes were 46, XY. He had no severe or recurrent infections and his immunoglobulin levels were normal. Now aged 8 years, he is toilet trained, speaks several meaningful words, but does not speak a two-word-sentence. He attends a primary school, and is affable and friendly. He is farsighted with astigmatism. He is able to run with a slow pitch and kick a soccer ball. He shows neither ocular apraxia nor cerebellar ataxia.

Patient 2, a boy, was born at 37 weeks of gestation to a 29-year-old mother and a 28-year-old father, both healthy and unrelated. The pregnancy was unremarkable. An older brother was healthy without malformations. Birth weight was 1560 g (−4.1 SD), length 39 cm (−5.9 SD), and head circumference 25 cm (−6.1 SD). At age 30 months, he sat alone but could not stand or walk. At age 5 years, he shuffled while sitting, but was unable to stand. At age 13 years, he weighed 9.2 kg (−4.2 SD), measured 97 cm (−7.0 SD), and had a head circumference of 35 cm (−12.8 SD). He had severe microcephaly, a bird-like face with sloping forehead, a big nose, large and simple ears, short palpebral fissures, a small mouth, and a small and receding chin. His shoulders, elbows, hips, and knees exhibited a decreased range of motion. Also noted were scoliosis, subluxation of the left elbow joint, bilateral cryptorchidism, and bilateral talipes equinus. His tendon reflexes were slightly exaggerated. G-banded chromosomes were 46, XY. His immunoglobulin levels were normal. Now aged 33, he lives in an institution for handicapped individuals. He does not speak meaningful words, but recognizes people, communicates by gesture, and shows fondness by touching. He is bedridden, is unable to roll over, and is handfed. He did not develop secondary sexual characteristics. He does not show ocular apraxia and had neither malignancy nor severe infections.

### 2.2. Immortalized skin fibroblast cells

Informed consent was obtained from Patients 1 and 2 and their families prior to this study. Primary skin fibroblast cells cultured from the two patients were immortalized by transfection with an SV40 virus and phTERT retrovirus vector [11]. We used as references immortalized fibroblast cell lines (designated as SVT) from various related disorders: NBS (GM7166VA7) [12], A–T (AT5BIVA) [13], and ATLD (D6807-SVT) [6,14]. A fibroblast cell line from a normal individual (SM-SVT) served as a control. A mouse hybrid cell line A9(neo11)-1 containing human chromosome 11 was provided by Dr. M. Oshimura, and microcell-mediated chromosome transfer was performed as previously described [12]. Fibroblast cell lines were maintained in D-MEM supplemented with 10% fetal bovine serum (Hyclone, Logan, UT, USA).

### 2.3. EB virus-transformed lymphoblastoid cell lines (LCLs)

LCLs were established from peripheral blood lymphocytes of the two patients and their family members. We used LCLs from NBS (94P247) [9], ATLD (200704L), and A–T as references, and a LCL from a normal individual (96-007M) as a control. A NBS cell line (94P247) was provided by Dr. K. Sperling. An ATLD cell line (200704L) was established from a blood sample from a boy with ATLD [15], supplied by Drs. S. Nonoyama and K. Imai. LCLs were cultured in RPMI 1640 with 20% fetal bovine serum.

### 2.4. Mutational analysis

PCR primers for *MRE11A* gene (GenBank NM_005591.3) were synthesized to amplify all coding exons and intron–exon boundaries [16]. PCR products were directly sequenced using an ABI

PRISM 3130 Genetic Analyzer (Applied Biosystems, Foster City, CA). RT-PCR primers were synthesized to amplify the *MRE11A* cDNA spanning exons 1–8 (5′-CGAAAAGAAGACAGCCTTGG-3′ and 5′-TCCAAAAATTGTTCTGGAATGA-3′) (GenBank NM_005590.3). RT-PCR products were visualized following electrophoresis on a 2% NuSieve agarose gel. PCR primers for *RAD50* (GenBank Z75311.1) and *NBN* cDNAs (GenBank AF058696.2) were synthesized to amplify the open reading frame with several overlapping segments.

Transcript levels of the *MRE11A*-c.338A and *MRE11A*-c.338G alleles in LCLs from a normal individual, Patient 2 and the parents were determined by the cycleave quantitative real time PCR assay (Cycleave-qPCR, TaKaRa Co. Ltd.) carried out in triplicate. Transcripts from the *HPRT1* allele were used as a quantification control. RNaseH sensitive fluorescent probes that specifically recognize the *MRE11A*-c.338A and *MRE11A*-c.338G alleles were used for the assay. The qPCR results were analyzed by the ΔΔCT method. qPCR primers and probes used for the assay are listed below.

MRE11A-F: 5′-ACGTTTGTAACACTCGATGAA-3′;
MRE11A-R: 5′-CTGGAATTGAAATGTTGAGG-3′;
MRE11Ac.338A: (Eclipse) 5′-dAdAdG(A)dTdGdGdCdAdA-3′ (FAM);
MRE11Ac.338G: (Eclipse) 5′-dAdAdG(G)dTdGdGdCdA-3′ (ROX);
HPRT1-F: 5′-CAGGCAGTATAATCCAAAGATG-3′;
HPRT1-R: 5′-ACTGGCGATGTCAATAGGA-3′;
HPRT1-probe: (Eclipse) 5′-dCdAdGdCdA(A)dGdCdT-3′ (FAM).

### 2.5. Western blot analysis

Western blotting was performed as described previously [17]. Primary antibodies used were: mouse anti-MRE11 monoclonal antibody (MRE11-12D7, 1:1000, GeneTex, Irvine, CA); mouse anti-RAD50 monoclonal antibody (13B3/2C6, 1:1000, GeneTex, Irvine, CA); rabbit anti-NBS1 polyclonal antibody (NB100-142, 1:500, Novus Biologicals, Littleton, CO); mouse anti-GAPDH monoclonal antibody (6C5, 1:1000, Santa Cruz Biotechnology, Santa Cruz, CA); and mouse anti-β-tubulin monoclonal antibody (1:2000, Sigma–Aldrich, St. Louis, MO).

### 2.6. Radiation-sensitivity analysis

Clonogenic analysis was performed on fibroblast cell lines to learn of their radiosensitivity as previously described [12]. Chromosome breakage analysis of LCLs was carried out as follows. Cells were irradiated with 2 Gy X-ray and harvested 24 h after irradiation. Giemsa-stained chromosome slides were prepared, and chromatid or chromosome breaks and quadriradials were counted.

### 2.7. ATM autophosphorylation after γ-irradiation

Immortalized fibroblast cells or LCLs were irradiated with 0.5 Gy of γ ray. At 15 min and 30 min after irradiation, the cells were analyzed with Western blotting using rabbit anti-ATM-p1981 monoclonal antibody (1:1000, Epitomics Inc., Burlingame, CA) and mouse anti-ATM monoclonal antibody (2C1, 1:1000, GeneTex, Irvine, CA). Band intensities were estimated using a densitometer and are presented as means ± standard deviation. The statistical differences were analyzed with Student's *t*-test. Statistical significance was assumed for $p < 0.05$.

### 2.8. DNA damage response assay

ATM-dependent G2/M checkpoint arrest was performed according to the methods described previously [18].

### 2.9. p53 phosphorylation after γ-irradiation

Lymphoblastoid cells were irradiated with 0.5 Gy of γ ray. At 15 min and 30 min after irradiation, the cells were analyzed with Western blotting using rabbit anti-phosphorylated p53 (Ser15) polyclonal antibody (1:1000, Cell Signaling Technology, Beverly, MA) and mouse anti-p53 monoclonal antibody (1:1000, Oncogene Research Products, CA).

### 2.10. Caspase 3 activation after γ-irradiation

Immortalized fibroblast cells were irradiated with 0 or 10 Gy of γ ray. At 72 h after irradiation the cells were analyzed with Western blotting using rabbit anti-cleaved caspase 3 monoclonal antibody (#9664, 1:1000, Cell Signaling Technology, Beverly, MA).

## 3. Results

### 3.1. Identification of MRE11A mutations

Several studies have demonstrated that microcephaly, as was present in the two patients we described, is a common feature in a variety of DNA damage repair defective disorders [2]. Therefore, we examined DNA damage repair proteins including ATM, ATR, MRE11, RAD50, and NBS1 in the two patients. Western blot analysis showed normal levels of ATM and ATR (data not shown) and reduced levels of MRE11, RAD50, and NBS1 in both patients (Fig. 2a). We, therefore, sequenced all the *MRE11A*, *RAD50*, and *NBN* coding sequences in both patients and found only the *MRE11A* mutations c.658A>C and c.659+1G>A in Patient 1, and c.658A>C and c.338A>G in Patient 2 (Fig. 2b). In Patient 1, c.658A>C was derived from the father, and c.659+1G>A from the mother. Two brothers were a heterozygote for c.659+1G>A. RT-PCR and sequencing analysis demonstrated that c.659+1G>A resulted in exon 7 skipping leading to a premature termination codon (p.Ser183ValfsX31) (Fig. 2c). The c.658A>C substitution located within exon 7 did not alter amino acids but affected splicing efficiency that resulted in exon 7 skipping (Fig. 2c). RT-PCR analysis of exons 1–8 of *MRE11A* cDNA from Patient 1 detected a reduced but considerable amount of correctly spliced transcripts in addition to the exon-skipped transcript (Fig. 2c). Western blot analysis of fibroblasts from Patient 1 detected a reduced amount of normal-sized MRE11 protein (Fig. 2a). No smaller-sized protein corresponding to the predicted truncated form was detected in both lymphocytes and fibroblasts. The c.658A>C substitution was not found in 100 normal Japanese individuals. These results indicated that the c.658A>C mutation leads to exon 7 skipping but that some of the RNA is correctly spliced.

Patient 2 was another compound heterozygote with c.658A>C, the same single-base substitution as the one found in Patient 1, and c.338A>G, a single-base substitution in exon 5. The c.658A>C substitution was inherited from the mother while c.338A>G was derived from the father. A DNA sample from the older brother was not available. Cloning and sequencing of the RT-PCR products of Patient 2 revealed two kinds of mRNA from the c.338G allele; normal sized transcripts carrying the c.338A>G substitution and intermediately sized transcripts resulting from exon 5 skipping (Fig. 2c). The normal sized products lead to an amino acid substitution of Asp to Gly at the 113th residue (p.Asp113Gly). The 113th residue is located within the highly conserved phosphoesterase domain, which is essential for endonuclease activity [19]. On the other hand, the intermediately sized transcripts resulting from exon 5 skipping lead to a premature termination codon (p.Phe106GlnfsX10). We then examined the levels of the transcripts from the c.338A and c.338G alleles by quantitative RT-PCR analysis. The correctly spliced

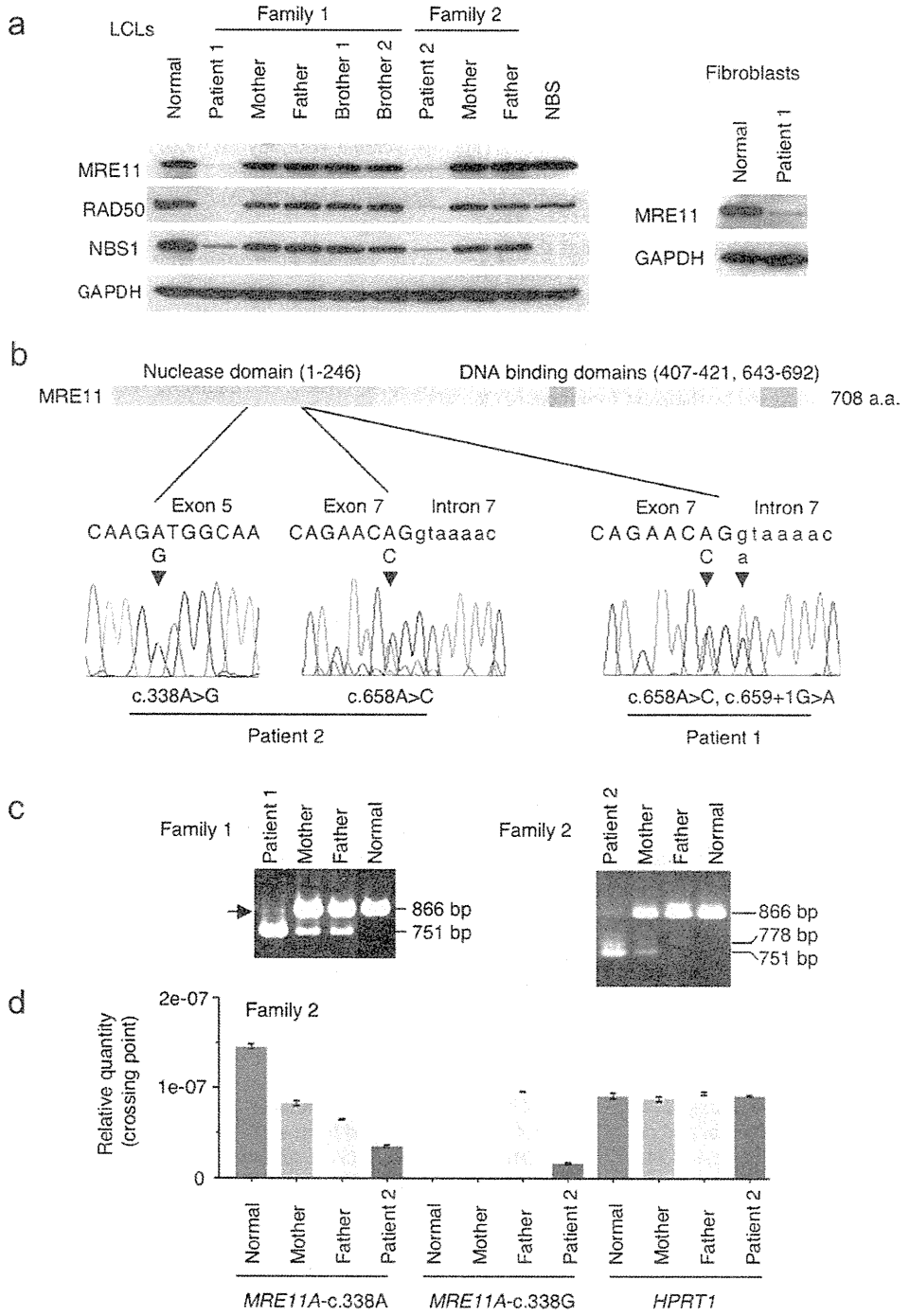


**Fig. 2.** MRE11 deficiencies associated with *MRE11A* mutations. (a) Western blot analyses of MRE11, RAD50, and NBS1 in lymphoblastoid cell lines (LCLs) from Patients 1 and 2 and their family members. Nijmegen breakage syndrome (NBS) cells were used as an NBS1-deficient reference, and anti-GAPDH antibody for equal loading. Levels of MRE11, RAD50, and NBS1 were reduced in both patients. Right panel shows a reduced MRE11 protein band of normal size in fibroblasts from Patient 1. (b) MRE11 protein structure and *MRE11A* mutations in Patients 1 and 2 as determined by genomic DNA sequencing. Patient 1 was a compound heterozygote with c.658A>C, a single-base substitution in exon 7, and c.659+1G>A, a substitution at an exon–intron junction of the splice donor-site. Patient 2 was a compound heterozygote with c.658A>C, the same single-base substitution in exon 7, and c.338A>G, a single-base substitution in exon 5. (c) RT-PCR analyses of exons 1–8 of *MRE11A* cDNAs from Patients 1 and 2 and their family members. RT-PCR of Patient 1 yielded two bands of 866 bp and 751 bp. The 866 bp band corresponds to the correctly spliced transcripts, and the 751 bp band to exon 7-skipped transcripts. The arrow on the left margin indicates the transcripts from the c.658A>C mutant allele. Analyses in the parents yielded two bands of 866 bp and 751 bp. RT-PCR of Patient 2 showed three bands of 866 bp, 778 bp, and 751 bp. The 866 bp band corresponds to the correctly spliced transcripts from the c.658A>C allele and the c.338A>G allele. The 778 bp band corresponds to exon 5-skipped transcripts, and the 751 bp band to the exon 7-skipped transcripts. (d) Quantitative RT-PCR analysis of the transcript levels from the c.338A and the c.338G alleles of Patient 2 and their family members. Transcripts from the *HPRT1* allele were used as a quantification control. The correctly spliced transcripts from the c.338G allele of Patient 2 showed 25% of the normal level. By contrast, the transcript levels from the c.338G allele of the father were not affected.

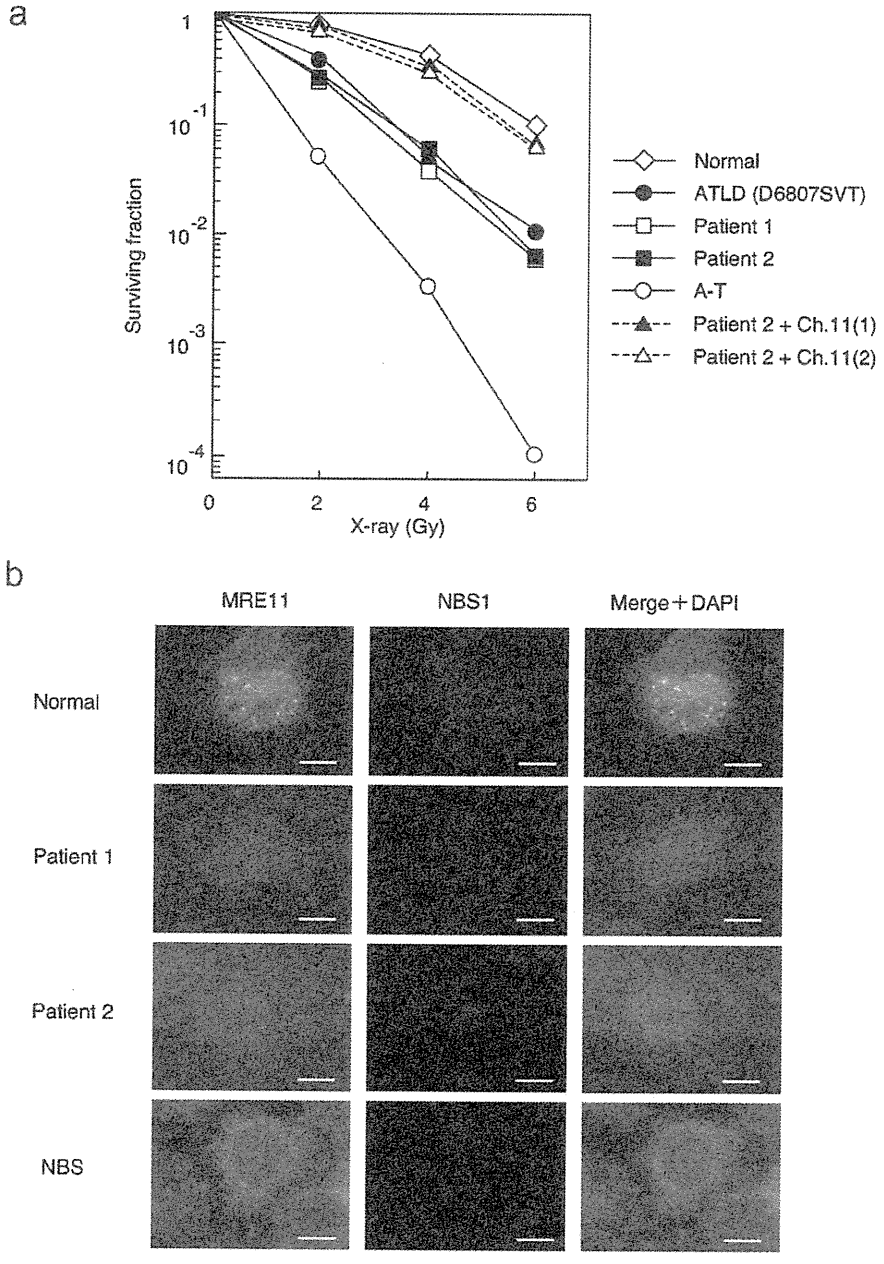


**Fig. 3.** Clonogenic survival curves for X-ray-irradiated fibroblasts. (a) Radiosensitivity was measured by counting colonies surviving radiation doses of 0–6 Gy. Colony survival was expressed as a logarithm. ATLD, ataxia–telangiectasia-like disorder; A–T, ataxia–telangiectasia. A–T cells were highly sensitive to radiation. Cells from Patients 1 and 2, and ATLD all showed intermediate levels of sensitivity. Microcell-mediated transfer of a human chromosome 11 (including the *MRE11A* locus) into the cells from Patient 2 restored radiation sensitivity. (b) Formation of MRE11 and NBS1 radiation-induced nuclear foci. Cells were analyzed by immuno-staining at 24 h after 6 Gy irradiation. Normal cells served as a control, and NBS cells served as an *NBN*-deficient reference. MRE11 and NBS1 formed nuclear foci after irradiation in normal cells. In contrast, cells from Patients 1 and 2 showed only very faint signals.

transcripts from the c.338G allele of Patient 2 showed 25% of the normal level (Fig. 2d). By contrast, the transcript levels from the c.338G allele of the father were not affected. The c.338A>G substitution was not detected in 100 normal Japanese individuals.

### 3.2. Cells from Patients 1 and 2 exhibit radiation-hypersensitivity

A clonogenic radiation sensitivity assay was performed on fibroblast cells from Patients 1 and 2 on ATLD and A–T cells as references, and on normal cells as a control. The cells from Patients 1 and 2, and ATLD were hypersensitive to X-ray irradiation, as measured by the share of surviving fractions after irradiation (Fig. 3a). A–T cells showed more marked radiation-hypersensitivity than in Patients 1 and 2, and ATLD. We introduced chromosome 11 (containing the *MRE11A* locus) into the cells from Patient 2 through microcell-mediated transfer [12]. Two microcell-hybrid clones obtained and both showed restoration of radiation-sensitivity (Fig. 3a).

Next, we studied MRE11 and NBS1 radiation-induced nuclear foci formation 24 h after exposure to 6 Gy. MRE11 and NBS1 formed nuclear foci after irradiation in normal cells. In contrast, cells from Patients 1 and 2 showed only very faint signals of NBS1 and MRE11. It is noteworthy that a few NBS1 foci were present in Patient 1. These findings are likely to be compatible with the level of the protein in the cells (Fig. 3b).